Doctoral Thesis in Technology and Health

Imaging and reconstruction of membrane proteins with cryoEM

QINGYANG ZHANG

KTH ROYAL INSTITUTE OF TECHNOLOGY

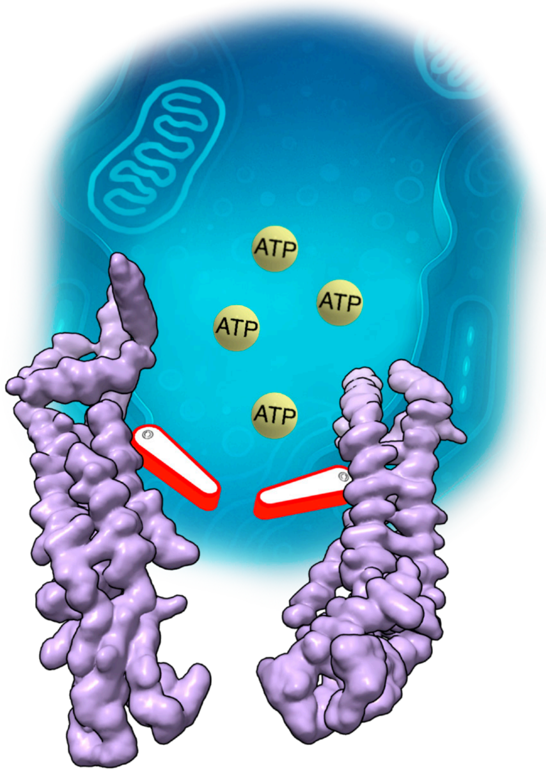

Imaging and reconstruction of membrane proteins with cryoEM

QINGYANG ZHANG

Academic Dissertation which, with due permission of the KTH Royal Institute of Technology, is submitted for public defence for the Degree of Doctor of Philosophy on Monday the 15th of December 2025, at 1:00 p.m. in Q2, Malvinas väg 10, Stockholm.

Doctoral Thesis in Technology and Health
KTH Royal Institute of Technology
Stockholm, Sweden 2025

TRITA-CBH-FOU-2025:37
ISBN 978-91-8106-487-2

Printed by: Universitetsservice US-AB, Sweden 2025

Abstract

Membrane proteins constitute 27% of the human proteome and play important roles in cellular processes. Dysfunction of membrane proteins causes and contributes to diverse diseases. The study of the structure and function of membrane proteins will help us to a deeply understand them. Cryo-electron microscopy (cryoEM) single-particle analysis (SPA) can provide us not only with high-resolution structures of membrane proteins but also give us the possibility to study protein's dynamics and heterogeneous complexes they form. In this thesis, we applied SPA together with electrophysiology, surface plasmon resonance (SPR) and Microscale thermophoresis (MST) to investigate the structural and functional properties of several membrane proteins and protein complexes.

In **Paper I**, we studied Pannexin 1 (PANX1), an ATP release channel involved in neurological disorders and inflammation. Electrophysiology and mass spectrometry identified Y308 as a key phosphorylation site. CryoEM structures revealed that phosphorylated PANX1 and the PANX1 R75A mutant possess conformational flexibility in the transmembrane domain. Our data show that PANX1 transits between a narrow and a wide state. This transition causes the N-terminal region to be ordered (wide) or disordered (narrow). The phosphomimetic Y308E mutant only shows a wide conformation with an ordered N-terminus. Electrophysiology shows this mutation converts PANX1 into a constitutively open channel. This suggests Y308 is a phosphorylation site that locks PANX1 into the wide conformation, enabling ATP release.

Paper II presents a modified workflow for identifying and determining the structures of membrane proteins in a heterogeneous sample; without prior knowledge of the protein sequence or a model. We used a conventional suing SPA workflow to obtain cryoEM maps. These maps were modelled unsupervised with ModelAngelo and a HMMER search was done to obtain sequence information. Our data allowed us to generate three different maps from a heterogenous sample. We were able to identify each protein only based on the maps. The results were supported by mass spectrometry. The three E. coli

membrane proteins were cytochrome bo3 oxidase (2.72 Å), AcrB (3.27 Å), and a previously uncharacterized *E. coli* ArnC protein (2.72 Å). Another important finding of this study is that MSP2N2 nanodiscs adapt their assembly around different proteins, implying that scaffold architecture depends on protein interactions.

In **Paper III**, we examined SMCT1 interactions with PDZK1. SMCT1 is an important membrane protein that transports monocarboxylate substrates like butyrate, lactate or niacin. It was thought that PDZK1 is an important regulator that influences the transport rate of SMCT1. We tested the affinity for SMCT1 with various assays. Our pull-down assay, SPR, and MST assays revealed only weak binding, suggesting the interaction is likely physiologically irrelevant except under conditions of local PDZK1 enrichment.

Overall, this work demonstrates the power of SPA for resolving dynamic membrane proteins, providing structural and functional insights, and establishing workflows for studying unknown or heterogeneous protein complexes.

Keywords:
Membrane protein, ion channel, transporter, pannexin 1 (PANX1), sodium coupled monocarboxylate transporter 1 (SMCT1), cryogenic electron microscopy (cryoEM), single particle analysis (SPA)

Sammanfattning

Membranproteiner utgör 27% av det humana proteomet och spelar viktiga roller i cellulära processer. Dysfunktion hos membranproteiner orsakar och bidrar till olika sjukdomar. Studiet av membranproteiners struktur och funktion kommer att hjälpa oss att förstå dem på en djupare nivå. Kryoelektronmikroskopi (cryoEM) med singelpartikelanalys (SPA) kan inte bara ge oss högupplösta strukturer av membranproteiner utan även möjliggör studier av proteindynamik och de heterogena komplex de bildar. I denna avhandling tillämpade vi SPA tillsammans med elektrofysiologi, ytplasmonresonans (SPR) och mikroskalig termofores (MST) för att undersöka de strukturella och funktionella egenskaperna hos flera membranproteiner och proteinkomplex.

I **Artikel I** studerade vi Pannexin 1 (PANX1), en kanal för ATP-frisättning som är inblandad i neurologiska sjukdomar och inflammation. Elektrofysiologi och masspektrometri identifierade aminosyran Y308 som en viktig fosforyleringsplats. CryoEM-strukturer avslöjade att fosforylerad PANX1 och PANX1 R75A-mutanter har konformell flexibilitet i transmembrandomänen. Våra data visar att PANX1 växlar mellan ett smalt och ett brett tillstånd. Denna övergång gör att N-terminalregionen antingen blir ordnad (bred) eller oordnad (smal). En fosformimetisk Y308E-mutant visar enbart en bred konformation med en ordnad N-terminus. Elektrofysiologi visar att denna mutation omvandlar PANX1 till en konstitutivt öppen kanal. Detta tyder på att Y308 är en fosforyleringsplats som låser PANX1 i den breda konformationen och möjliggör ATP-frisättning.

Artikel II presenterar ett modifierat arbetsflöde för att identifiera och bestämma strukturerna av membranproteiner i ett heterogent prov, utan förkunskaper om proteinsekvensen eller en modell. Vi använde ett konventionellt SPA-arbetsflöde för att erhålla cryoEM-kartor. Dessa kartor modellerades oövervakat med ModelAngelo och en HMMER-sökning gjordes för att få sekvensinformation. Våra data gjorde det möjligt för oss att generera tre olika kartor från ett heterogent prov. Vi kunde identifiera varje protein enbart baserat på kartorna. Resultaten stöddes av masspektrometri. Bland de många

proteiner som identifierades fanns de tre E. coli-membranproteinerna cytochrom bo3 oxidas (2.72 Å), AcrB (3.27 Å), och ett tidigare okarakteriserat E. coli ArnC-protein (2.72 Å). En annan viktig upptäckt i denna studie är att MSP2N2-nanodiskar anpassar sin sammansättning runt olika proteiner, vilket antyder att ställningsarkitekturen beror på proteininteraktioner.

I **Artikel III** undersökte vi SMCT1-interaktioner med PDZK1. SMCT1 är ett viktigt membranprotein som transporterar monokarboxylat-substrat som butyrat, laktat eller niacin. PDZK1 har ansetts vara en viktig regulator som påverkar transporttakten hos SMCT1. Vi testade affiniteten för SMCT1 med olika assay. Våra pulldown-, SPR- och MST-assays tyder dock på att bindningen är mycket svag och sannolikt fysiologiskt irrelevant utom under förhållanden med lokal PDZK1-anrikning.

Sammanfattningsvis demonstrerar detta arbete kraften i SPA för att lösa dynamiska membranproteiner, ge strukturella och funktionella insikter, och etablera arbetsflöden för att studera okända eller heterogena proteinkomplex.

Nyckelord
Membranprotein, jonkanal, transportör, pannexin 1 (PANX1), natriumkopplad monokarboxylattransportör 1 (SMCT1), kryoelektronmikroskopi (cryoEM), singelpartikelanalys (SPA)

Translated by deepseek

List of publications:

This thesis is based on the following articles. Full versions of the articles are appended at the end of the thesis.

i. Zhang, Q., Wang, J., Gaullier, G., Kotol, D., Blikstad, C., Dahl, G., Barro-Soria, R. & Mim, C. (2025). Structural basis of ATP release and ion selectivity in Pannexin1 channels. bioRxiv, 2025-02.

ii. Zhang, Q., Murthy, A. V., & Mim, C. (2025). In silico classification and identification co-purified protein complexes yield new structures and multiple MSP assembly states. bioRxiv, 2025-02.

iii. Zhang, Q., Clinton, J., Westerlund, K., & Mim, C. (2025). SMCT1 has a low affinity to PDZ domain containing 1 protein. Micropublication Biology, 2025, 10-17912.

Author contribution

i. Production and purification of the protein, cryoEM data collection, SPA data processing, figure generation, writing draft

ii. Production and purification of the protein, sample preparation for MS, cryoEM data collection, SPA data processing, writing draft

iii. Production and purification of the protein, performing SPR and MST, data analysis, writing draft

List of abbreviations:

GPI	Glycosylphosphatidylinositol
ArnC	Undecaprenyl-phosphate 4-deoxy-4-formamido-L-arabinose transferase
SMCT	Sodium-coupled monocarboxylate transporter
PDZK1	PDZ domain containing 1
P2X7R	P2X purinoceptor 7
PSD-95	Postsynaptic density protein 95
NMDAR	N-methyl-D-aspartate receptor
nNOS	Neuronal nitric oxide synthase
UDP	Uridine diphosphate
ATP	Adenosine triphosphate
ADP	Adenosine diphosphate
NAD^+	Nicotinamide adenine dinucleotide
LRRC8	Leucine-rich repeat-containing 8
CALHM	Calcium Homeostasis Modulator
PANX	Pannexin
Cx	Connexin
cryoEM	Cryogenic electron microscope
GLUT	Glucose transporter
AcrB	Acriflavine resistance protein
RedOx	Reduction-oxidation

H^+	Hydrogen ion
Na^+	Sodium ion
K^+	Potassium ion
ATPase	Adenosine triphosphatase
MCT	Monocarboxylate transporter
SLC	Solute carrier
LMNG	Lauryl maltose neopentyl glycol
E. coli	*Escherichia coli*
RNAP	RNA polymerase
HSP	Heat shock protein
PTM	Post-translational modification
CHO	Chinese hamster ovary
Sf9	*Spodoptera frugiperda 9*
HEK	Human embryonic kidney
GFP	Green fluorescent protein
SDS-PAGE	Sodium dodecyl sulphate polyacrylamide gel electrophoresis
WB	Western blot
SMALP	Styrene maleic acid lipid particle
CMC	Critical micelle concentration
SDS	Sodium dodecyl sulphate
DDM	N-dodecyl-β-D-maltoside

GDN	Glyco-diosgenin
MSP	Membrane scaffold protein
LC-MS/MS	Liquid Chromatography-Tandem Mass Spectrometry
TEVC	Two-electrode voltage clamp
MST	Microscale thermophoresis
SPR	Surface plasmon resonance
NMR	Nuclear magnetic resonance spectroscopy
TROSY	Transverse relaxation-optimized spectroscopy
TEM	Transmission electron microscope
CCD	Charge-coupled device
DED	Direct electron detector
2D	Two dimension
3D	Three dimension
MicroED	Microcrystal electron diffraction
cryoET	Cryogenic electron tomography
SPA	Single-particle analysis
kDa	Kilodalton
Fab	Antigen-binding fragment
Nb	Nanobody
Mb	Monobody
PSF	Point spread function

CTF	Contrast transfer function
FSC	Fourier shell correlation
GPU	Graphics Processing Unit
IMAC	Immobilized metal affinity chromatography
BO3	Cytochrome bo 3 ubiquinol terminal oxidase
MBP	Maltose binding protein
KD	Dissociation constant
SD	Standard deviation
SMA	Styrene maleic acid

Table of Contents

1 Membrane proteins

The cell membrane functions as a selective barrier that defines the boundaries of the cell, maintaining internal homeostasis while allowing communication and exchange with the external environment [1], [2]. The membrane consists mostly of phospholipids, cholesterol and membrane proteins [2].

Membrane proteins constitute 27% of the human proteome and play important roles in cellular processes, such as cell signalling (receptors), enzyme catalysis, membrane scaffolding and solute and macromolecular transportation (transporters and channels) [3]. Dysfunction of membrane proteins causes and contributes to diverse diseases, such as amyotrophic lateral sclerosis (Glutamate transporter 1) [4], schizophrenia (glycine transporters) [5], and cancer (Sodium-coupled monocarboxylate transporter 1) [6]. For these reasons, there is a lot of interest to study membrane proteins.

Membrane proteins themselves can be classified based on their structural features, namely as integral, including lipid/ Glycosylphosphatidylinositol (GPI) anchored proteins, and peripheral membrane proteins (Fig.1) [7], [8]. In this PhD thesis, I focus on integral membrane proteins with multiple transmembrane helices (alpha helices).

Generally, membrane proteins can also be classified functionally, namely as scaffold proteins, structural/adhesion proteins, enzymes, transporters and ion channels (Fig. 2) [9]–[16]. Depending on the perspective, some membrane proteins belong to more than one group. In the following section, I will briefly introduce each class and give examples for each class. This will serve also as an introduction to the membrane proteins I investigated in this PhD thesis.

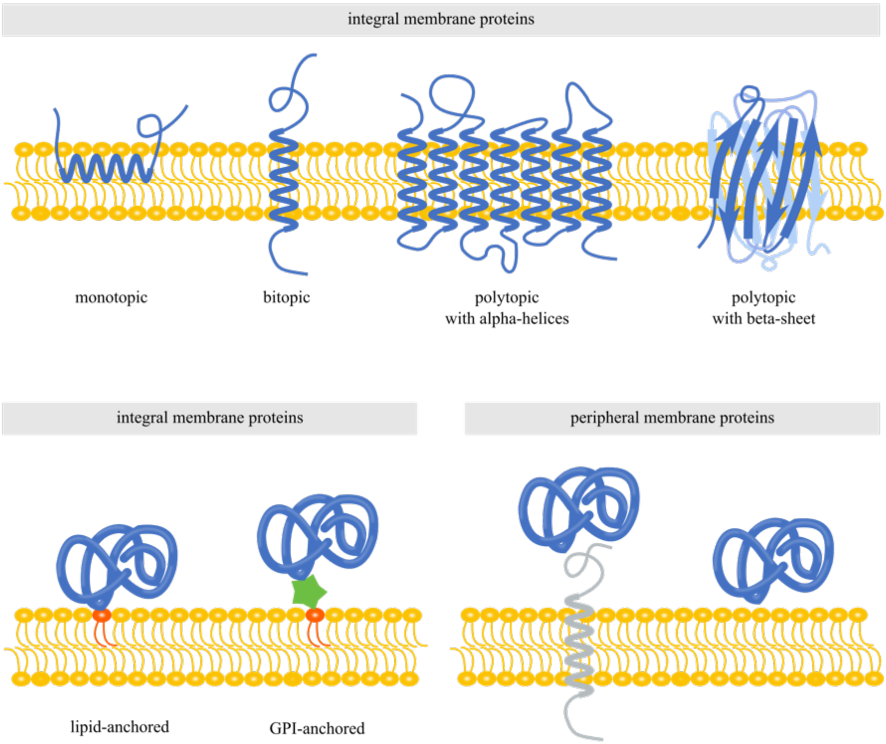

Figure 1. Schematic illustration showing two categories of membrane proteins based on their structures: integral membrane proteins and peripheral membrane proteins. Integral membrane proteins include proteins with transmembrane domains, lipid-anchored proteins and GPI-anchored proteins. Based on the topology of transmembrane proteins, it can be further divied into monotopic when protein only embeds into one side of the membrane; biotopic when protein crosses the membrane and has only one transmembrane domain; polytopic when protein crosses the membrane several times. Peripheral membrane proteins are proteins associated with the membrane surface through membrane or other transmembrane protein. Membrane proteins are indicated in both blue and grey; the blue ones represent those in each category. The yellow circles with two tails are membrane lipids, and the red ones represent lipids that interact with membrane proteins or GPI (green stars).

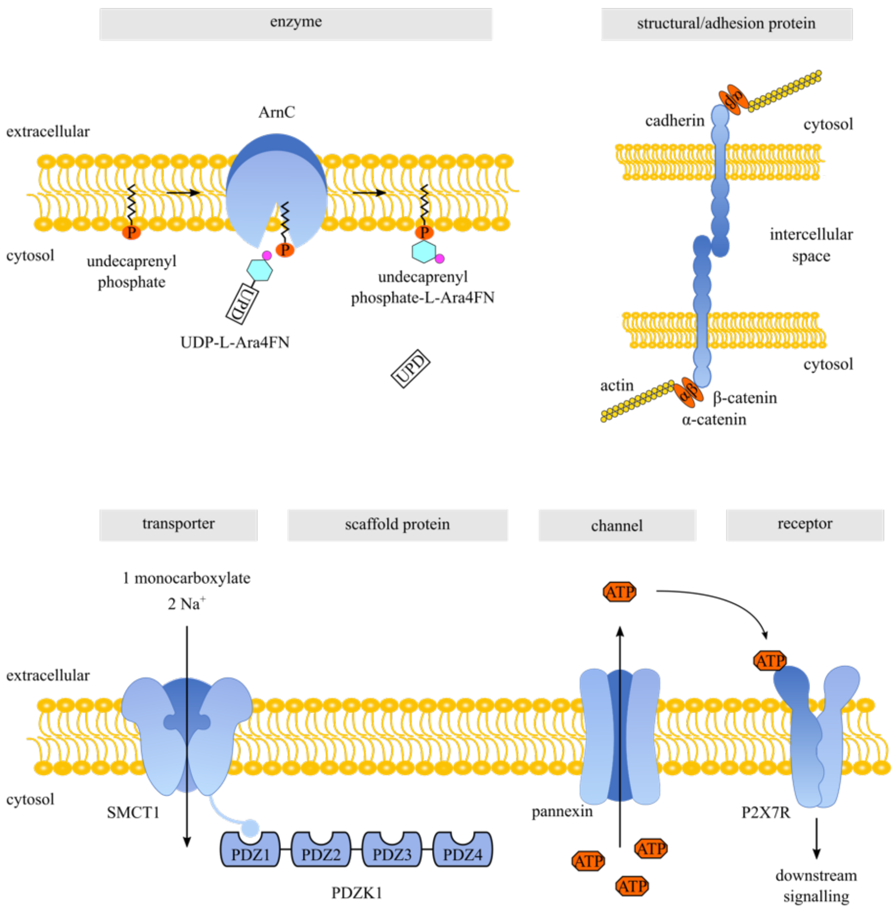

Figure 2. Representative examples of an enzyme, Undecaprenyl-phosphate 4-deoxy-4-formamido-L-arabinose transferase (ArnC); a structural/adhesion protein (cadherin); a transporter, the Sodium-coupled monocarboxylate transporter 1 (SMCT1); a scaffold protein, PDZ domain containing 1 (PDZK1); a channel, Pannexin 1; and a receptor, the P2X purinoceptor 7 (P2X7R) are illustrated (P2X7R is a channel as well). Most of the proteins shown here were subject of the PhD thesis. The illustration also shows that membrane proteins need to work together to accomplish their function in cells. Membrane proteins are indicated in blue. The yellow circles with two tails are membrane lipids

1.1 Scaffold proteins

Scaffold proteins act as an assembling platform for proteins, and cluster membrane proteins, often found in cell signalling. Scaffolding proteins not only bring receptors and enzymes together, thereby facilitating their interactions, but also control their localization in the cell.

Postsynaptic density protein 95 (PSD-95) is one of most thoroughly studied scaffolding proteins in the excitatory synapse, where it binds to receptors, enzymes and other scaffold proteins [17], [18]. For instance, PSD-95 binds to both the N-methyl-D-aspartate receptor (NMDAR) and the neuronal nitric oxide synthase (nNOS) to form a complex. In this way, it couples NMDAR-mediated calcium flux with nNOS activation [19].

One of the proteins I investigated in this study, SMCT1, contains a PDZ binding motif as well. PDZ Domain Containing 1 (PDZK1) binds to SMCT1 through this PDZ binding motif and increases its substrate uptake (Fig. 2) [12], [20].

1.2 Structural/adhesion proteins

Cell adhesion proteins help cells to adhere to each other and the extracellular matrix; examples are cadherin, integrin and nectin [21], [22]. All three of them are integral membrane proteins with a single transmembrane helix [22], [23].

Cadherin is worthwhile to highlight, because it plays an important role in tissue morphogenesis and tumor suppression [24]. Figure 2 illustrates cadherin binding between two cells. The extracellular domain of cadherin is responsible for binding to another cadherin molecule on an adjacent cell, whereas the cytoplasmic domain protein-proteins interactions are involved in signalling pathways [23].

1.3 Enzymes

Enzymes are proteins that catalyze a chemical reaction. The most common enzymes found in membrane are oxidoreductases, transferases, hydrolases, lyases, isomerases and ligases[3].

The Undecaprenyl-phosphate 4-deoxy-4-formamido-L-arabinose transferase (ArnC) is an example for a modifying enzyme. It is one of the proteins described in paper II. ArnC catalyses the transfer of 4-deoxy-4-formamido-L-arabinose from uridine diphosphate (UDP) to undecaprenyl phosphate (Fig. 2). The modified arabinose (which is positively charged) is then attached to lipid A (the lipid moiety in lipopolysaccharide) to reduce the negative charge of the outer bacterial membrane. This makes bacteria resistant to polymyxin (positively charged) and cationic antimicrobial peptides [14], [25].

1.4 Receptors

A receptor is a protein that receives a signal via binding to a ligand and initiates a cellular response. In this thesis, I will focus on membrane receptors. Membrane receptors play a key role in communication between the cell and its external environment.

The most common membrane receptors are G protein-coupled receptors, ligand gated ion channels and receptor tyrosine kinases [26]. G protein-coupled receptors are the largest receptor family, with around 800 members in humans [27], [28]. In short, upon ligand binding to G-protein-coupled receptor, they activate a G-protein (through dissociation into α-subunit and βγ-subunit complex). The released G-protein triggers downstream signalling pathways such as neurotransmission, immune response and hormonal regulation by activation of proteins, like the adenylyl cyclase [28], [29].

Receptor tyrosine kinases trigger downstream signalling pathways by phosphorylating themselves and target proteins [30]. Ligand gated ion channel receptors, like the adenosine triphosphate (ATP) activated P2X7R receptors (Fig. 2), allow the flow of ions along the electrochemical gradient between both sides of the membrane in response to a ligand [16].

1.5 Ion channels and transporters

The cell membrane is mostly impermeable to small, charged and polar molecules, like metabolites and ions. Yet, there are three ways to transport small molecules (carbohydrates, amino acids, nucleosides, and ions) across membrane with the help of a dedicated protein [1].

First, passive diffusion through a pore/channel; second; facilitated diffusion through a transport protein; and third active transport through a transport protein. Facilitated diffusion needs no external source of energy because molecules travel along their concentration gradient. On the other hand, active transport requires energy, because this mode transports a substrate against its concentration gradient.

1.5.1 Ion channels

Ion channels are membrane proteins, which allow ions (like K^+, Na^+, Cl^-, or Ca^{2+}) to pass through membrane by following their electrochemical gradient [1], [11], [31]. Based on the channel activation mechanism, ion channels can be gated by various stimuli, including ligands, voltage, mechanical stimulation or even light [11], [31], [32]. Once a channel is activated, it undergoes conformational changes and opens a aqueous pore to allow specific ions to pass through [33].

In addition to their mode of activation, ion channels can also be classified according to their ion selectivity. Some ion channels are highly ion-specific (e.g., sodium channel or potassium channels), while others like NMDA receptors are permeable to multiple ions, including Na^+, Ca^{2+}, and K^+ with different permeabilities [33].

Among the various ion channel families, large pore channels have the broadest spectrum of ion permeability. In addition to small ions, these channels also permeable to larger molecules, such as ATP, adenosine diphosphate (ADP), nicotinamide adenine dinucleotide (NAD^+), and glutamate [34]. These molecules serve as signalling molecules and play important roles for physiological responses.

Connexins were the first members of large-pore channels to be discovered. They can be activated by voltage, pH, and extracellular Ca^{2+} [35]–[37]. There are more than twenty connexin isoforms and with various stoichiometries [38], [39]. Nevertheless, all connexin share similar structure with four transmembrane domains per monomer. Six monomers assemble to form a hemichannel and two hemichannels from adjacent cells form a gap junction.

Structural studies of connexins have shown that the gating of connexins involves both electrostatic and steric factors [34]. Calcium binds to the extracellular region of connexins and changes the electrostatics of the protein, thereby mediating gating [40], [41]. The N-terminal region also serves as a gate and moves dynamically in the pore between open and close conformations [42].

After connexin, additional large-pore channels were discovered, including innexin, pannexins, leucine-rich repeat-containing 8 (LRRC8) and calcium homeostasis modulators (CALHM) [34]. Although these channels share similar functional properties (permeable to large molecules, like ATP), their sequences have little homology [43].

Despite their sequence variability and the subunit length, the transmembrane helices are arranged in a highly similar topology across these families (with four transmembrane helices per monomer) [44]–[48]. But the oligomer states are different among them (range from 6-mers to 13-mers). This structural variability influences their gating properties, pore size, and selectivity. Notably, CALHM channels can form oligomers ranging from 8-mers to 13-mers [48].

1.5.1.1 Pannexin 1

ATP is generally considered the ‘energy currency’ inside the cell, but it also plays a crucial extracellular role as a signalling molecule in a process known as purinergic signalling [49], [50]. ATP binds to purinergic receptors P2 (P2X and P2Y) on the cell surface to activate its downstream signalling pathway and thereby regulating cellular functions, such as cell proliferation, growth and development, immune and inflammatory responses, neuropathic pain [49]–[51].

Given the importance of extracellular ATP signalling, understanding how ATP is released from cells becomes crucial. ATP can be released either passively from necrotic cells or actively and controlled through vesicular exocytosis and various ion channels (e.g. connexin, pannexins, CALHM1) [43].

Pannexins (PANX) are major ATP release channel. Pannexins were first identified by homology search for gap junction [52]. There are three members of Pannexin family (PANX1-3). PANX1 is the most ubiquitously expressed and studied protein in its family [43].

Due to its role in ATP release PANX1 has been increasingly recognized as a key player in multiple pathological conditions, including breast cancer, melanoma, stroke, epilepsy, inflammation, and chronic pain [53], [54]. Inhibition of PANX1 suppresses tumour growth and metastasis and relieves inflammatory responses and neuronal hyperexcitability [55], [56].

These findings highlight the importance of understanding how PANX1 can be specifically inhibited. There are already few inhibitors for PANX1 include probenecid, carbenoxolone, brilliant blue FCF [56], [57]. However, many of them are also inhibitors for other channels and transporters. For example probenecid can also inhibit other organic anion transport channels, and carbenoxolone is known to block PANX2 as well as multiple connexins, affecting both gap junctional and hemichannel activity [58], [59].

For this reason, the structural study of PANX 1 at different states could provide more information for rational drug design. Such as, probenecid was found not simply block the channel but instead may stabilize PANX1 in a non-resting closed conformation [60]. Understanding how different compounds bias PANX1 toward specific functional states can inform the rational design of conformation-selective modulators with improved specificity and therapeutic potential.

Before the release of cryo-EM structures, PANX1 was widely misclassified as a hexameric protein. This misconception arose largely from the limitation of biochemical methods used to characterize Panx1. native-PAGE, which is imprecise at high molecular weights, makes it difficult to distinguish between hexameric and heptameric assemblies. However. in 2020, six independent groups [46], [61]–[65] have released their PANX1 cryo-EM structures and all of them show PANX1 is a heptameric ion channel (Fig. 3) [46].

All current structures confirm earlier functional studies that the narrowest part of the pore is formed by a tryptophan at residue 74 (in both human and mouse). The extracellular W74 is believed to be the size selective gate for substrates [64], which is unique for PANX1. Neither PANX2 or PANX3 have a tryptophan in this position [66], [67]. Depending on the method to determine the substrate passing through PANX1, molecules up to 1 kDa can pass PANX1 with ATP being the most important one [68], [69]. W74 also forms cation-π interaction with R75 on the adjacent chain (Fig. 3), which provide the basis for anion selectivity for PANX1 [65]. Although the structures shed light on the architecture of PANX1, a knowledge gap remains about the activation mechanism of ATP conduction [70].

PANX1 has at least 3 different states, the closed, the small pore (low conductance, Cl^- specific) and large pore (high conductance, ATP release) state. The small pore conformation is activated by voltage stimulation and at that conforamtion, it only conducts Cl^- [71], [72].

There are several ways to activate the large pore state, which can release ATP and other large molecules, like the positively charge molecule YoPro [53]. One stimulus is mechanical force on the cell membrane [73], another stimulus is intracellular calcium or extracellular potassium [74], [75]. Last, proteolytic cleavage of the distal C terminus [46], [68], application of lysophospholipids [76] and phosphorylation by the Src family kinase have been shown to activate the ATP permeability [77].

Caspase cleaved PANX1 has been proposed to release ATP and the pore has been proposed to be large enough for ATP to pass [46]. However, structural comparison raises doubt about this proposal [70].

Although caspase cleavage activates PANX1, this process is irreversible and typically occurs during apoptosis. Therefore, the measured ATP could have its origin from dying cells [78]. It is unlikely that proteolysis represent the main physiological activation mechanism when ATP release is reversable. Therefore, phosphorylation mediated activation may potentially provide a reversible activation mode for PANX1, which needs further investigation, as explored in Paper I.

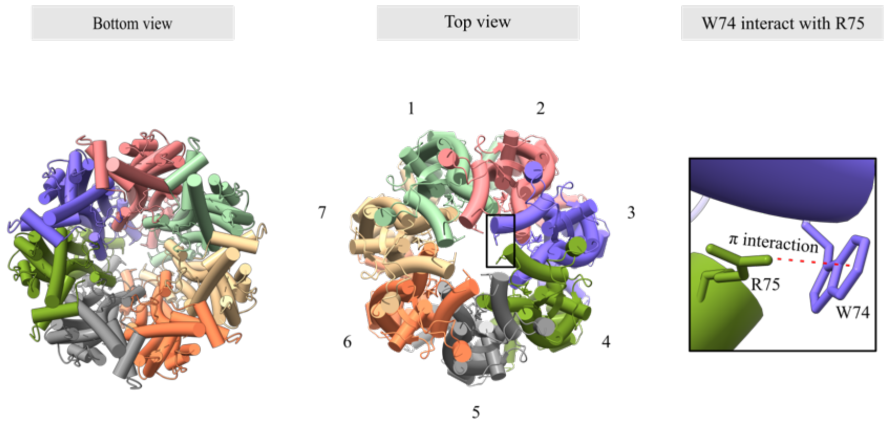

Figure 3. CryoEM structure of wide type PANX1 (6WBF). Both bottom view and top view of PANX1 structure shows it is a heptamer. Zoom in view of W74 interacting with R75 on its adjacent chain and form a cation-π interaction (red dash line).

1.5.2 Transporters

Transporters are membrane proteins, which transport ions, peptides, small molecules, lipids, and big molecules across the cell membrane. Based on the transportation method, transporters can be divided into: Passive transporters/facilitated diffusion/carrier proteins, meaning the molecule is transported along its concentration gradient without additional energy; Active transporters, meaning the molecule is transported against the concentration gradient by using some form of energy [1].

Examples of passive transporters are glucose transporter (GLUT) family glucose transporters, that transport glucose from the extracellular space into the cell without any need of energy [79]. The energy for active transport is usually provided by ATP hydrolysis (primary active transport) or the electrochemical gradient of co-transported substrates (secondary active transport) [80]. Examples are ion pumps that transport ions across the membrane by hydrolysis of ATP [80]. An example for co-transport of ions is the multidrug efflux pump subunit AcrB (Acriflavine resistance protein B) that transports drugs outside the cell by counter transport of H^+ into the cell [81]. Another example is the Sodium-coupled monocarboxylate transporter 1 (SMCT1) which transports monocarboxylates into the cell by cotransport of 2 Na^+ into the cell [15].

The substrate transport from the extracellular space to the cytosol can be simplified by a transport cycle with a minimum of three states: an outward facing, occluded and inward facing state (Fig. 4) [82]. In the outward facing state, the transporter presents its high affinity binding sites to substrates on the outside. Once substrates bind to the transporter a conformational change is induced which will end access of the transporter to the outside side: the occluded state. Next the transporter will change its conformation with the binding sites for the substrate facing the opposite side. The substrate affinity in this state decreases and causes the substrates to be released from the transporter (inward facing). The substrate release will cause another conformational change and reverting the transporter to present the binding sites to face outwards, thereby resetting the transporter to its original state [82], [83].

The transport cycle is in principle reversable, because it is coupled to electro-chemical gradient across the membrane [82]. This is important when the gradient changes, e.g. if a cell dies. This cycle is essential for the controlled movement of molecules across cell membranes, allowing cells to maintain homeostasis and perform critical physiological functions. The structural study of each state in the transportation cycle is important to understand transporter function in health and disease [84].

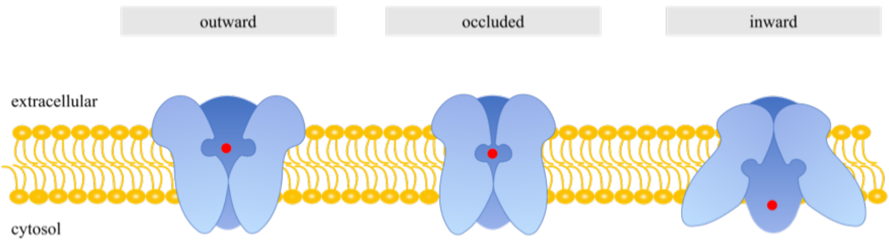

Figure 4. Schematic representation of the transportation cycle: outward-facing, occluded, and inward-facing. Membrane proteins are indicated in blue. The yellow circles with two tails represent membrane lipids. Ligand binding (red dot) triggers conformational changes that mediate substrate translocation across the membrane.

1.5.2.1 Sodium-coupled monocarboxylate transporter 1

Monocarboxylic acids are a broad class of small molecules like metabolites such as lactate, pyruvate, ketone bodies or nutrients like vitamin B3. These molecules play essential roles in the cellular metabolism, particularly as alternative energy sources and signalling molecules [85], [86].

The transport of these acids is achieved by two transport systems: sodium independent monocarboxylate transporter (MCT, belonging to the solute carrier (SLC) 16 family); and the sodium dependent monocarboxylate transporter (SMCT, belonging to SLC5 family) [85], [87], [88]. Unlike MCTs, which functions via proton coupling, SMCTs use the sodium gradient to drive transport [88]. There are two members in SMCT family, SMCT1 and SMCT2 [88].

SMCT1 is expressed in the brain, where it transports lactate and ketone bodies into neurons as energy source [87]. Other than in the brain, SMCT1 is abundantly expressed in colon, kidney and thyroid. In colon, it absorbs short chain fatty acids; in kidney it reabsorbs lactate acid and nicotinate; in thyroid, it releases iodide [88]. SMCT1 expression is silenced by DNA methylation in colon cancers and *smct1* was later identified as a tumour suppressor gene [6]. The SMCT1 substrate butyrate is an inhibitor of histone deacetylase (HDAC), which decreases the acetylation level of histone, alters the structure of chromatin (closed chromatin), and in turn changes gene expression [89], [90].

As mentioned earlier SMCT1 is an active transporter. It transports one monocarboxylate together with 2 Na^+ ions into the cell, which generates one net positive charge per cycle. Currently there is only one structure of SMCT1 stabilized by Lauryl maltose neopentyl glycol (LMNG) detergent in an inward facing state, presumably in complex with butyrate [91].

Studying the structure of SMCT1 in different states and in complex with various substrates or inhibitors would provide valuable insights into its transport mechanism and the molecular determinants of substrate recognition and inhibition.

2 Sample preparation of membrane proteins

Portions of membrane proteins' primary sequence are hydrophobic. The translation machinery recognizes these and insert these into the membrane. This fact presents a challenge that cytosolic or secreted proteins do not have [92], [93].

Integral membrane proteins need to be stabilized, and the hydrophobic parts needs to be shielded from the aqueous environment, when investigated in isolation [94]. Further, depending on their origin, these proteins may have post-translational modifications and require a specific insertion machinery [95]. This restricts the options how to produce the membrane protein. Here I will present several strategies for membrane protein preparation.

2.1 Choice of the protein expression host

Producing sufficient membrane proteins is essential to study their biophysical and biochemical properties. While some membrane proteins can be extracted directly from organisms in which they are naturally abundant (endogenous sources), many proteins of interest require overexpression in a heterologous host system (exogenous sources) [96]–[98]. These expression systems are broadly classified into two categories based on the host organism: prokaryotic systems and eukaryotic systems (including yeast, insect, and mammalian cells) [98], [99].

2.1.1 Prokaryotic expression systems

The bacterium *Escherichia coli* (*E. coli*) is one of the most frequently used host to produce recombinant membrane proteins, due to well-established protocols, cost-efficiency, and ease of genetic manipulation. This system offers rapid growth rates and inexpensive media, making it particularly appealing for large-scale protein production [100], [101].

In *E. coli*, membrane proteins are first translated and then targeted, inserted, and folded into the cytoplasmic membrane. Specialized *E. coli* expression strains, such as C41 and C43, have been developed from BL21 (DE3) to enhance the yield of potentially toxic proteins and membrane proteins with slowing transcription of T7 RNAP (RNA polymerase) [102], [103]. Other strategies, including low-temperature expression, slow protein synthesis allow proper folding [104]. Additionally, osmotic stress, e.g. induced by adding sorbitol to the growth medium, can increase the expression of heat shock proteins (HSPs), which assist in protein folding [105]–[107]. Signal peptides like the pelB signal from *Erwinia carotovora* can also be introduced to facilitate protein translocation across the membrane [108].

Despite its advantages, the *E. coli* system has several limitations. It lacks the lipids, molecular chaperones, and the post-translational modification (PTM) machinery required for proper folding and function of many eukaryotic membrane proteins [92]. Also, the codon usage difference between organisms is a problem [92]. Although numerous modifications have been made to address these shortcomings, *E. coli* remains unsuitable for proteins requiring complex PTMs. As such, alternative host systems are often necessary for producing eukaryotic membrane proteins.

2.1.2 Eukaryotic expression systems

Compared to prokaryotic systems, eukaryotic hosts are more complex, expensive, and time-intensive to maintain [109]. However, they provide significant advantages, including the ability to perform complex PTMs like glycosylation, which is critical for the localization and function of certain proteins [109], [110].

Yeasts, such as *Saccharomyces cerevisiae* and *Pichia pastoris*, are the most widely used eukaryotic host. Yeast systems share many benefits with *E. coli*, including rapid growth rates, ease of genetic manipulation, and scalability [111]. Additionally, yeasts can perform some eukaryotic PTMs, such as disulfide bond formation (in bacteria this happens in the periplasm), phosphorylation, acylation, prenylation, and limited O- and N-linked glycosylation. These modifications are essential for proper folding, activity, and membrane insertion of certain proteins [112], [113]. However, glycosylation patterns in yeast differ across strains and rarely match native mammal/vertebrate patterns [114], [115].

Insect cell systems, such as the *Sf9* cell line derived from *Spodoptera frugiperda* ovaries, are another popular choice for protein expression. These systems offer several advantages, including the ability to perform extensive PTMs and glycosylation patterns that are closer to mammalian cells. It also has a translocation machinery closer to mammalian cells, plus the chaperones [116]–[118]. *Sf9* cells are commonly used with baculovirus-mediated expression systems and have proven successful for expressing proteins requiring complex modifications [46], [116], [119]–[121].

For membrane proteins that demand specific PTMs and unique subcellular environments, mammalian cell lines (like Chinese hamster ovary (CHO) cells and human embryonic kidney (HEK293) cells) are the preferred expression system [122], [123]. These systems are particularly suitable for producing functional mammalian proteins, as they provide the native folding and PTM machinery required for many proteins to be active [124], [125].

2.1.3 Cell-free systems

An alternative to cellular expression systems is the use of cell-free platforms, which allow *in vitro* protein translation. These open systems utilize translation machinery derived from cell lysates of various organisms [126]. Cell-free systems are versatile and enable precise control over reaction conditions, offering a powerful tool for producing proteins that are challenging to express in traditional host systems and for specific labelling of amino acids [127]–[129].

2.2 Protein purification

A reason to use exogenous produced proteins is the ease to genetically engineer a purification tag to enrich the protein. Recombinant proteins can be designed with an affinity tag at the N or C-terminal end so the protein can be captured on chemically modified resins. The most used affinity tags is the His-tag (with 6 His amino acid added to the target protein). However, many proteins can bind to immobilized metal ion chromatography resins, like Nickel-NTA column non-specifically [130]–[132].

There are many other affinity tags with higher specificity, such as the Strep-tag (Strep-Tactin resin), the GST-tag (glutathione-coupled resin), the AVI-tag (streptavidin, avidin resin or anti-AVI-tag antibody-conjugated resin) and biotin-tag (avidin or streptavidin resin). Aside from affinity tags, recombinant proteins can carry tags that improve solubility, assist protein export or help to monitor the protein production.

The GFP-tag (green fluorescent protein) is frequently used to monitor the protein expression and purification. In addition, GFP is stable enough to retain its fluorescence in SDS-PAGE (Sodium dodecyl sulfate polyacrylamide gel electrophoresis), which saves time compared to a western blot (WB) to identify the protein.

Size exclusion chromatography is typically performed at the end of the purification to verify the homogenous state of the protein and to remove protein aggregates and other impurities based on protein size [133].

To enrich endogenous proteins, one would have to generate a specific antibody that targets the endogeneous protein or use other physico-chemical methods to enrich the protein (ultracentrifugation, ion exchange chromatography, etc).

2.3 Membrane protein extraction and solubilization

As mentioned above, membrane proteins need to be stabilized when they are removed from the membrane. In principle there are two options to extract membrane proteins: detergent extraction or direct extraction (e.g., utilizing SMALPs [Styrene maleic acid lipid particle]) (Fig. 5).

Detergent extraction is the most widely used method for solubilizing membrane proteins. Detergents are amphipathic molecules that contain both hydrophobic and hydrophilic regions. The hydrophilic "head" interacts with water molecules via hydrogen bonding, while the hydrophobic "tail" interacts with the protein's hydrophobic regions during solubilization [97]. Detergents are classified based on the nature of their hydrophilic head group into three categories: ionic (anionic or cationic), non-ionic, and zwitterionic [97].

Ionic detergents are highly effective but are often too harsh for membrane protein solubilization due to their ability to disrupt protein-protein interactions [97]. For instance, sodium dodecyl sulfate (SDS), an anionic detergent, is efficient for solubilizing membrane proteins but is generally denaturing [134], [56]. Some proteins, such as bacteriorhodopsin, can be renatured by transferring them from SDS to a suitable lipid or non-denaturing detergent environment [137].

Non-ionic detergents are milder compared to ionic detergents, as they primarily disrupt lipid-lipid and lipid-protein interactions without significantly affecting protein-protein interactions [97]. This property makes them more suitable for membrane protein solubilization [97], [138]. Common non-ionic detergents include DDM (n-dodecyl-β-D-maltoside), LMNG (Lauryl Maltose Neopentyl Glycol) and GDN (Glyco-diosgenin).

Zwitterionic detergents possess both positive and negative charges on their head group, combining properties of ionic and non-ionic detergents [97]. However, like ionic detergents, zwitterionic detergents can disrupt protein-protein interactions, making them less ideal for solubilizing membrane proteins.

Beyond their chemical classification, an important physico-chemical property of all detergents is the critical micelle concentration (CMC), the minimum concentration at which detergent molecules aggregate to form micelles [139]. For effective solubilization, the detergent concentration in the buffer must exceed the CMC [140].

The effectiveness of a detergent for solubilizing a membrane protein is difficult to predict and often requires an empirical approach. Different detergents may show varying success depending on the type of integral membrane protein. Previous research has highlighted preferences for certain detergents in specific applications [138], [141]. Therefore, optimizing detergent selection often involves a trial-and-error process to determine the most suitable conditions for solubilization and stabilization, including detergent, ionic strength, buffer components like ions, pH etc.

After solubilization, membrane can be kept in detergent during the purification. Many detergents allow for imaging by cryoEM, especially, detergent with lower CMC, such as GDN and LMNG [134], [142].

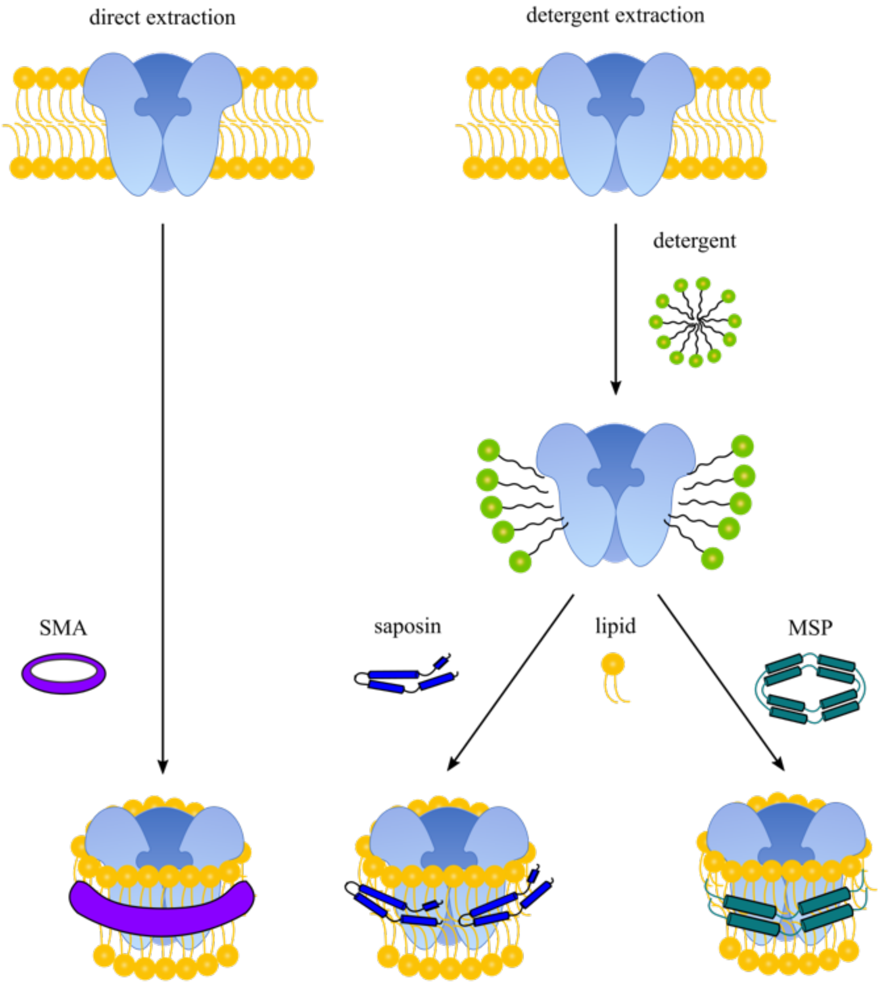

Figure 5. Three different methods of membrane protein extraction and stabilization are shown. Left panel direct extraction method, where SMA (styrene maleic acid) is used to extract membrane proteins from the cell membrane together with the surrounding membrane lipids directly. For this method, no additional lipids are needed. Right panel membrane proteins are first solubilized in detergent, then saposin or MSP (membrane scaffold protein) is used to form a nanodisc with the membrane protein and additional lipids. The yellow circles with two tails represent both the membrane lipids and the lipids added later.

2.4 Membrane model systems

The cell membrane is not a passive carrier for membrane proteins. The opposite is true, in many cases membrane proteins like ion channels or transporters actively interact with lipid species [143]–[146]. Therefore, it is interesting to incorporate the lipid membrane into the investigated samples.

Various methods have been developed to incorporate extracted membrane proteins into model membranes to preserve their native structure and activity. One example is liposomes, which are self-enclosed lipid vesicles composed of a lipid bilayer. Many membrane proteins have been successfully reconstituted in liposomes [147]–[149], but controlling protein orientation remains a challenge [150]. Nanodiscs offer a potential solution for some of these challenges associated with other model membrane systems [150].

Nanodiscs are disc-shaped structures composed of membrane scaffold proteins (MSPs) and phospholipids, providing a native-like lipid environment that enhances membrane protein stability [151]–[153]. MSPs are derived from apolipoproteins for nanodisc formation and engineered to produce nanodiscs of varying diameters, typically between 9 and 17 nanometers [155], [156].

The assembly of nanodiscs begins by solubilizing phospholipids and MSPs in a detergent mixture. Upon detergent removal—through dialysis or styrene beads (Bio-Beads) adsorption—a nanodisc self-assembles, forming a phospholipid bilayer domain encircled by MSPs in a belt-like configuration [154].

The appropriate MSP and the optimal ratio of membrane protein, lipid, and MSP are selected based on the size and characteristics of the target membrane protein [152], [155]. This setup allows for customizable lipid composition, which is critical for studying protein-lipid interactions [152].

The advantage of nanodiscs is the ability to keep membrane proteins in an aqueous solution, while they are in a native-like lipid environment [151], [152]. However, a limitation of nanodiscs is that they may constrain the structure of some membrane proteins [157] and manuscript II.

In addition to MSPs, saposin, a small lysosomal protein, can also form nanodiscs [158]. Unlike MSPs, saposin adapts to a variety of membrane protein sizes by various stoichiometries around the membrane protein to form the nanodisc structure [159].

Like saposin, styrene maleic acid lipid particles (SMALPs) are polymers composed of styrene and maleic acid group at various ratios that surround the lipids [160]. It has various size as MSPs. The advantage of direct isolation is that it perseveres native protein lipid interactions [161].

2.5 Protein identification

We need to ensure that the purified protein is the desired protein. A widely used method for protein identification is SDS-PAGE followed by Western blotting. However, additional information about post-translational modifications (PTMs), such as glycosylation and phosphorylation, is sometimes required. Although PTM-specific antibodies can be generated for WB applications, this approach is time-consuming, costly, and may lack specificity [162]–[164].

Mass spectrometry-based bottom-up proteomics offers a valuable alternative for both protein identification and PTM analysis [165], [166]. In traditional bottom-up proteomics, protein fragmentation is achieved by using enzymatically digestion before undergoing LC-MS/MS (Liquid Chromatography-Tandem Mass Spectrometry) analysis. Software is then used to identify the sequence of the peptides to reconstruct the original protein by matching the identified peptides to a comprehensive proteomic database [167], [168].

3 Functional and structural studies of membrane proteins

Functional studies of membrane proteins represent a challenge, and some functions can only be studied with asymmetric conditions between cytosolic and extracellular part. In the following I present several methods to study their function and structure.

3.1 Functional methods

3.1.1 Electrophysiology

The cell membrane is formed by lipids, which functions as barrier to keep ions and other charged and polar molecules from moving freely between compartments [2]. For charged molecules, the concentration difference across the membrane creates an electrochemical potential [11], [169]. Membrane proteins that allow ions to pass across the membrane close the circuit and allow us to measure the potential, current and conductance.

Ion channels are the simplest case to create a connection between the inside and outside of the cell: when the channel (e.g. pannexin) opens, ions can pass and create a current depending on their electrochemical gradient [44], [170]. The same is true for a transporter if a transporter (e.g. SMCT1) moves a net charge across the membrane, also known as electrogenic [171], [172]. This movement of ions generates currents across the cell membrane and changes the electric potential. A special case are transient currents, when charges are moved temporarily, e.g.

only steps of the transport cycle move charges, or charged substrates/parts of the protein move and relax into a new state [173].

Electrophysiology is a collection of methods that can measure electrical properties in biological systems [174]. For single cell electrophysiology, a cell is placed in a bath and a glass micropipettes are used to measure electric properties. The electrodes are positioned so that membrane proteins close the circuit (Fig. 6a) [175], [176]. There are many different configurations to measure electric properties, often one electrode is placed inside the cell. This way it can measure the current and potential change of the whole cell. Most commonly, electrical properties of proteins in cells are measured under constant conditions [174], [176].

There are two ways to set up an electrophysiology experiment, one is current clamp, the other is voltage clamp. In the current clamp method, the amplifier maintains a constant current and by applying and measuring the membrane potential needed to maintain the current. On the other hand, voltage clamp measures the current necessary keep the membrane potential constant [176]. Variations of the clamp technique are patch clamp, where a tight seal is formed between the electrode and cell membrane and the two-electrode voltage-clamp [176]–[178].

Two-electrode voltage clamp (TEVC) (Fig. 6b) is a common electrophysiological technique used to control the membrane potential (Vm) of large cells to study the properties of electrogenic membrane proteins, especially ion channels [178][175]. TEVC uses two intracellular electrodes—a voltage electrode as Vm sensor and a special current electrode for current injection to adjust the Vm. The membrane potential at desired values is maintained by a differential amplifier, which records the membrane current as well. To analyse ion channel properties, we not only see when a channel opens, measured by a change of resistance, but we also know how much current goes through it at different conditions. TEVC is necessary, because of the large currents that need to be injected, due to the size of the experimental system like giant axons or large cells, such as *Xenopus* oocytes. *Xenopus* oocytes are often used to study the function of exogenous expressed ion channels and receptors, since its membrane has low expression of endogenous channels and receptors. Exogenous proteins are expressed by injecting DNA or RNA into oocyte. The bath composition is adjusted to test different ligands or ion permeability.

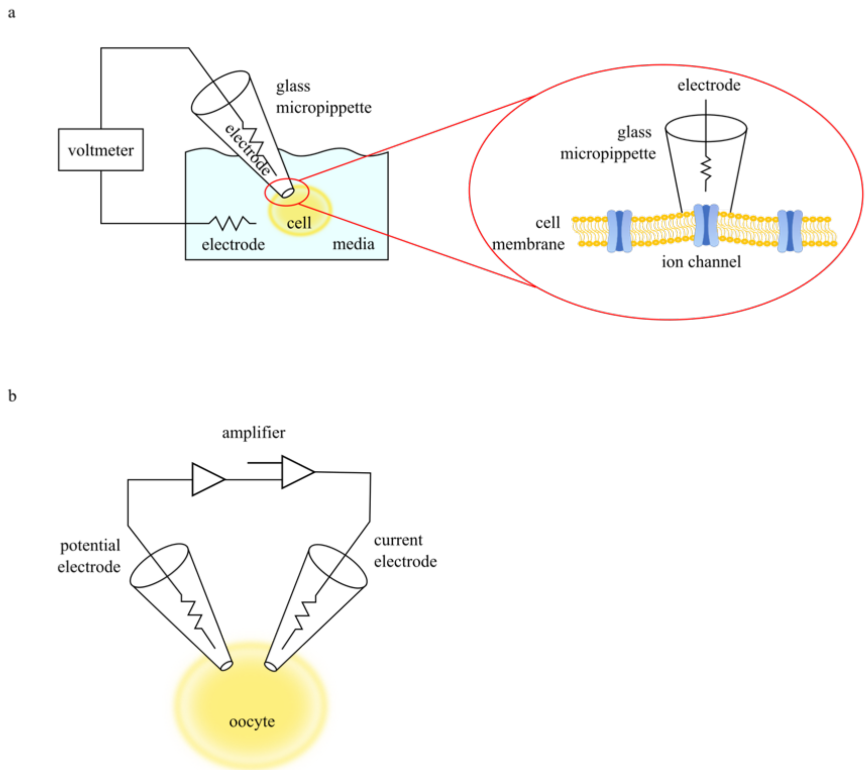

Figure 6. Electrophysiology setups. (a) Schematic illustration of a voltage-clamp configuration, in which membrane potential is held constant while measuring current through membrane proteins. (b) Two-electrode voltage clamp (TEVC) setup, commonly used in large cells such as *Xenopus* oocytes to record ion channel or transporter activity under controlled conditions.

3.1.2 Methods to study protein interactions

Protein–protein interactions play essential roles in biological processes. As mentioned in section 1.1, PDZK1 has been described to bind to SMCT1 through its PDZ binding motif and increases substrate uptake [12].

There are many ways to study protein interactions, qualitatively by Western blot, or co-immunoprecipitation; and quantitively by microscale thermophoresis (MST) and Biacore™ surface plasmon resonance (SPR).

MST is a fluorescence-based biophysical technique and measures the temperature-induced change in fluorescence. This change can be caused by temperature related intensity change of the fluorescent probe and movement of fluorescent labelled protein (thermophoresis). Both of them will be affect by binding events [179]. The reduction of the fluorescence is proportional to the concentration of potential binding partner (non-fluorescent labelled) if the fluorescently labelled and the unlabelled protein interact (Fig. 7). MST allows measurement of interactions directly in solution without the need of immobilization to a surface.

Biacore™ SPR measures biomolecular interactions by a change in refraction index caused by mass change when potential binding partner binds to the immobilized protein on sensor surface (Fig. 8) [180]. It does not require a label but a need to immobilize one of the interacting proteins onto the sensor surface.

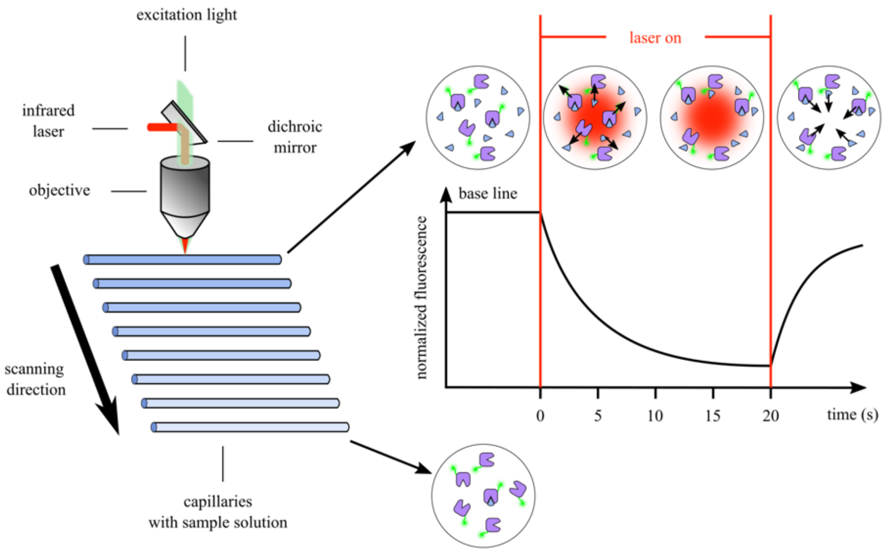

Figure 7. Schematic representation of Microscale Thermophoresis (MST). Capillaries are loaded with sample mixture containing a fluorescently (green) labelled protein (purple). Each capillary has a different concentration of a non-labelled partner (blue). Laser induced temperature change and causes the movement of proteins. The instrument records the fluorescence intensity over the time. The intensity change correlates with the concentration-dependent binding of the non-labelled partner.

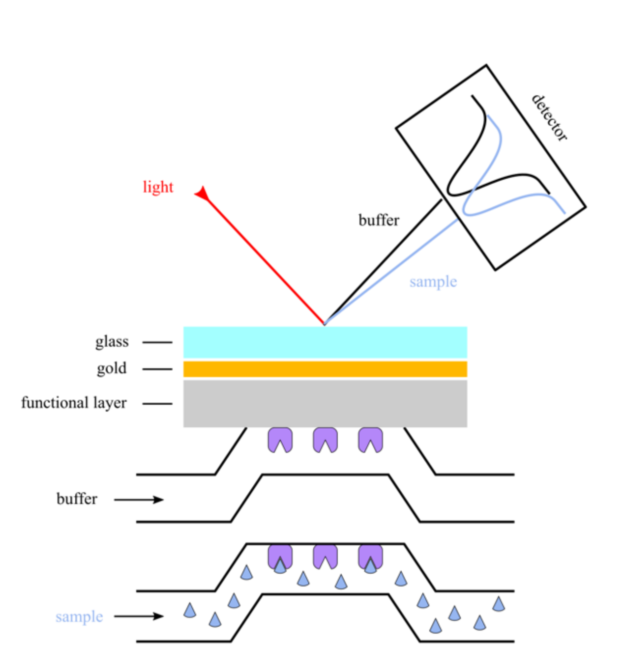

Figure 8. Schematic representation of Biacore™ Surface Plasmon Resonance (SPR). The protein (purple) is immobilized on the surface of the chip. When its binding partner (blue) flows past the chip surface, it will bind to the protein. The causes a change in the refractive index at the sensor surface and is recorded by the detector.

3.2 Structural methods

3.2.1 X-ray crystallography

X-ray crystallography provides high-resolution, three-dimensional structural information of proteins, often at atomic detail, and is considered a fundamental technique in structural biology. It requires the protein to form ordered crystals. Exposure of the crystal to an x ray beam causes a diffraction pattern (Fig. 9). The spacing in the crystal lattice causes constructive and destructive interference which creates these patterns. The diffraction patterns can be used to back calculate structural information about the protein [181].

The challenge in x-ray crystallography is to form ordered protein crystals, which is difficult for membrane proteins. One of the reasons is that the detergents and membrane mimetics surrounding the transmembrane part of membrane proteins, leave a small surface area (loops and hydrophilic region) for it to form crystal contacts. Also, it is often difficult to produce large amount of membrane protein that is stable over a long time to form crystals.

Various crystallization techniques exist, such as, liquid-liquid diffusion methods, crystallization under dialysis and vapor diffusion technique [181], [182]. *In meso* crystallization/ lipid cubic phase is a method developed to overcome the obstacles associated with crystallizing detergent-solubilized transmembrane proteins [183], [184].

All crystallization methods require empirical determination of parameters like protein concentration, precipitating agents, pH and temperature [181], [182]. The use of commercial crystal screen kits and automation (mosquito®) reduced labour and speeds up the process [185]. Currently, around 80% of structures in the PDB database are from x-ray crystallography (chart 1) [186].

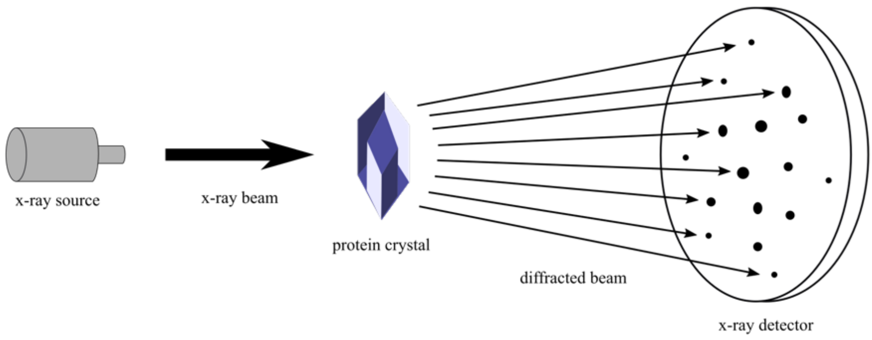

Figure 9. Schematic representation of an X-ray crystallography setup. The X-ray beam is generated from the X-ray source and passes through the protein crystal. The beam is diffracted by the protein crystal, forming a diffraction pattern that is captured by the X-ray detector. This diffraction pattern is used to determine high-resolution protein structures.

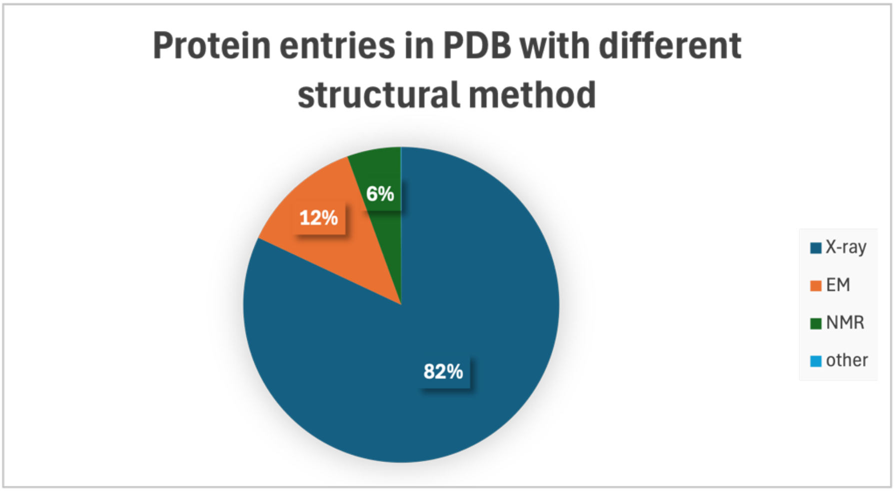

Chart 1. Protein entries in PDB with different structural method. Around 82% of the protein entries in PDB is from X-ray crystallography, 12% from EM, 6% NMR and very few from other methods.

3.2.2 Nuclear magnetic resonance spectroscopy

Nuclear magnetic resonance spectroscopy (NMR) is another technology to obtain protein structures. It uses the phenomenon that nuclei align with a strong constant magnetic field. An oscillating magnetic field (in the radio frequency range) causes the nuclei to change their orientation. Once the signal is switched off, the nuclei relax into their initial state and produce an electromagnetic signal with a frequency characteristic of the magnetic field at the nucleus. This signal is characteristic for the chemical environment around the nucleus and can be used to identify chemical components and their interactions [187].

Not all nuclei are NMR active, and proteins used for NMR study may need to be isotope labelled, which adds an additional challenge during expression (minimum media reduce the yield) and cost (isotope labelled media) [188]. The protein-induced signal is relatively weak, so high sample concentrations are required [189].

Unlike x-ray crystallography, NMR also provides dynamic information of a protein. The limiting factor for NMR is the protein size. It is difficult to interpret spectra if the proteins larger than 30kDa [190].

There are new technical developments to try to break the size limitation, including NMR spectrometers with increased experimental sensitivity, and specific isotope labelling and TROSY (Transverse relaxation-optimized spectroscopy)-type experiments [191].

3.2.3 Transmission Electron microscopy

The electron microscope was invented in 1931 by Ernst Ruska and Max Knoll [192][193]. It can use either backscattered electrons for imaging the surface of a sample, known as scanning electron microscope (SEM) or transmitted electrons for imaging the internal structure of a sample, known as transmission electron microscope (TEM) [194].

A schematic of an electron microscope is illustrated in figure 10 [195]. In general, a transmission electron microscope (TEM) consists of an electron source (or gun) at the top, which emits electrons that are accelerated and focused by a series of electromagnetic lenses. The electron beam then passes through a thin specimen, and the transmitted electrons are further focused to form an image on a detector at the bottom of the column. The entire system operates under high vacuum to allow electrons to travel freely [193].

With technological advancements in the electron sources and detectors, TEM has seen significant improvements [196]. Early electron microscopes used traditional thermionic (heat-emission) guns, which were later replaced by more stable and brighter cold field-emission guns [197]. Similarly, image recording progressed from photographic film to CCD (charge-coupled device) cameras (which were sometimes used in parallel with film), and eventually to direct electron detectors (DEDs), which significantly enhanced image quality [198].

Because biological samples are sensitive to radiation damage and vacuum conditions, special precautions must be taken. One solution was negative stain, which envelops biological samples with a coat of heavy metal salt and makes the specimens beam resistant, but the stain limits the resolution [199]. One option is embedding the sample into a sugar to make the sample vacuum resistant without the resolution limitation of negative stain [200].

The development of methods for freezing biological samples in liquid ethane, to produce non-crystalline (vitreous) ice for imaging, revolutionized high resolution TEM. The preservation in vitreous ice (Fig. 10) not only makes the sample more resistant beam damage and vacuum, but also maintains the protein structure close to its native state. This breakthrough laid the foundation for cryo-electron microscopy (cryoEM) [201], [202]. In 2017, the Nobel Prize in chemistry was awarded to three biophysicists, Jacques Dubochet, Joachim Frank, and Richard Henderson, for their pioneering contributions to the development of cryoEM for the high-resolution structure determination of biomolecules.

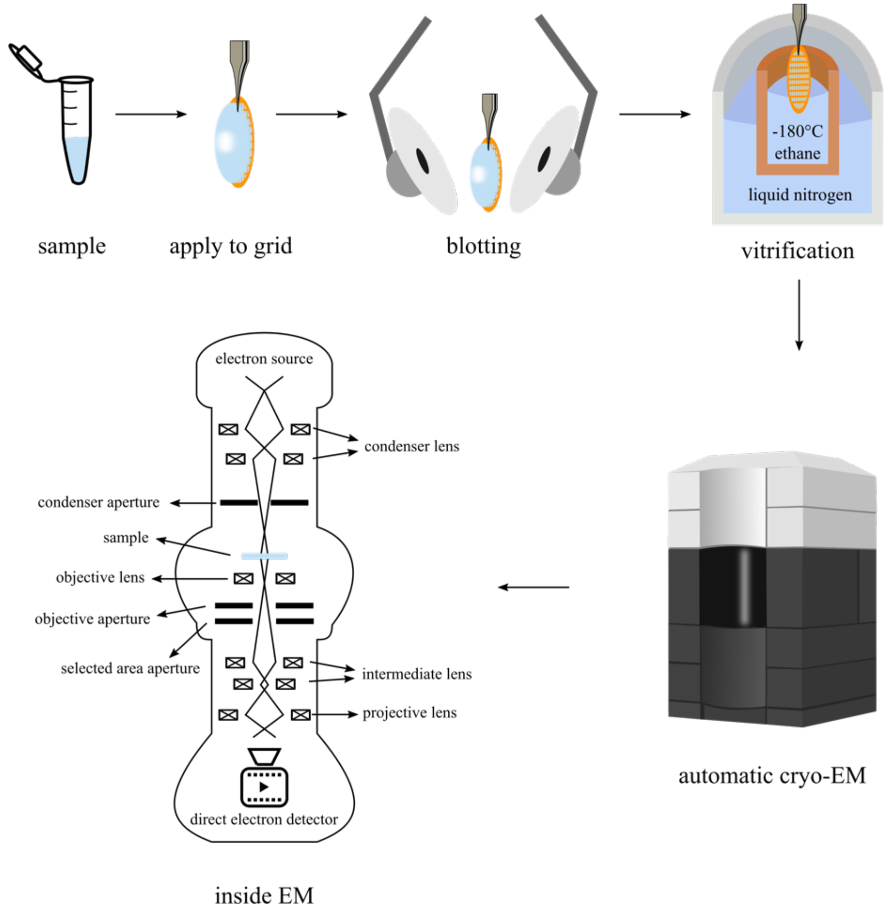

Figure 10. Schematic representation of cyroEM grid preparation and electron microscope setup. Protein sample is applied onto the grid and extra liquid is blot away before vitrification. Vitrification is performed with liquid ethane at -180°C cooled by liquid nitrogen. Nowadays, the grid is transferred into an automatic sample handling mechanism inside the microscope, which still contains same key components of a transmission electron microscope, including the electron source, lenses, specimen stage, and detector.

3.2.3.1 Cryogenic Electron Microscopy

CryoEM can also be used in different modes. In microcrystal electron diffraction (MicroED), the TEM magnifies the diffraction patterns in the back focal plane (around one of the intermediate lenses) [203]. Like x-ray crystallography, crystallization is the bottleneck of this technique, but small crystals are easier to obtain than larger crystals [203]. Until 2025, there are around 272 PDB entries from MicroED [186].

So far, I discussed protein structure generated *in vitro*. Although, proteins themselves are in near-native states in vitreous ice, studying proteins directly in cells with cryogenic electron tomography (cryoET) preserves more of their native environment. Also, single objects like nucleus and Golgi apparatus can be imaged [204], [205]. In cryoET we generate different images of the object by tilting the sample. The knowledge of the imaging angle can be used to reconstruct the 3D structure. Although the typical resolution of cryoET is around 20Å [206], recent publications show, that resolutions observed in single-particle analysis (SPA) can be achieved by subtomogram averaging [207]–[209].

SPA which is the method used in this thesis, will be discussed in the next section.

4 CryoEM single particle analysis

Single particle analysis has evolved into the dominant technique in cryoEM, and is the technique used to solve the structures of the protein complexes in this thesis. For this technique we are recording the images of individual proteins and protein complexes. In this chapter I will describe some considerations to get an 3D object from an image (Fig. 11).

As a necessity, thousands of 2D images of the sample must be recorded from all angles. The angular sampling is achieved imaging the sample in randomly spread orientations or by tilting the specimen (if the particle images show preferred orientation).

Computational algorithms align these 2D images to increase the signal to noise ratio through averaging. Those aligned images together with determined angles are used to reconstruct a 3D volume of the sample (Fig. 11). The initial 3D model is refined to get more accurate angles and shifts to increase resolution. This allows for detailed visualization of the molecular structure. Information about the workflow can be found in the following subsections.

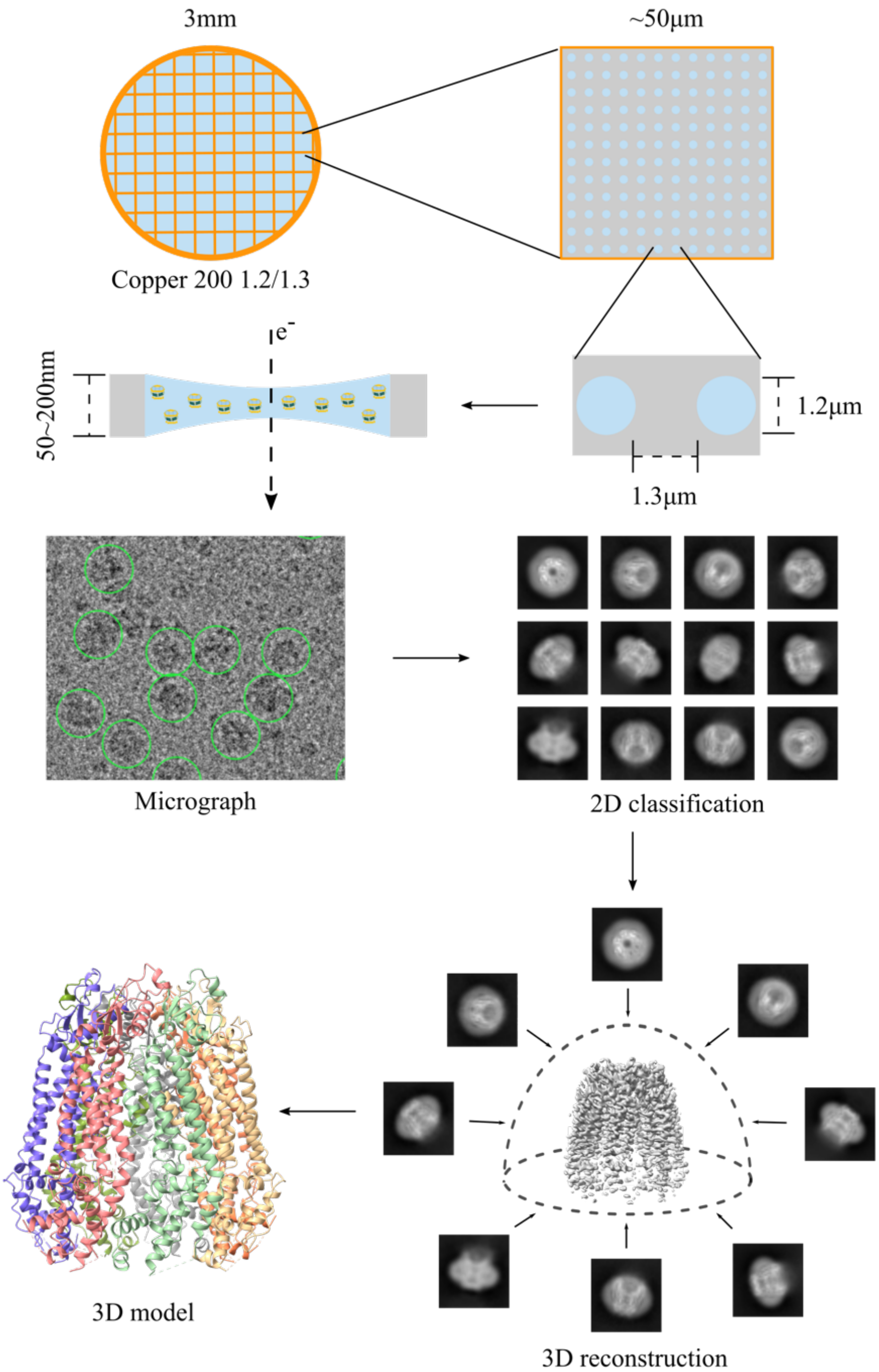
3mm
~50µm
Copper 200 1.2/1.3
e-
50~200nm
1.2µm
1.3µm
Micrograph
2D classification
3D model
3D reconstruction

Figure 11. Schematic representation of the cryo-EM grid and single-particle analysis workflow. (Top) This shows a copper grid (200 1.2/1.3), where each square contains a carbon layer. The carbon layer has holes with defined diameters and spacing. Images (micrographs) are collected from the holes filled with frozen solution containing protein samples. Dark spots on the micrographs, which resemble proteins, are selected as particles. Particles with the same orientation are grouped together to form 2D classes. Through 3D reconstruction, the angles and shifts between particles are determined. A 3D model of the protein is then built based on the 3D structure.

4.1 CryoEM SPA sample preparation

Sample preparation is important step during cryoEM. Protein size, sample purity, homogeneity, ice thickness and grid choice can all effect the final results.

4.1.1 Increasing protein size and protein stability

SPA is well suited for proteins larger than 100 kilodaton (kDa), the smaller proteins are, the less likely is it that a project will be successful, especially for non-symmetric proteins smaller than 50 kDa. A straightforward way to increase the sample size is a complex of the target protein with an interaction partner. If the protein does not have a suitable interaction partner, because either the affinity is not high enough or the interaction partner is too flexible, it is possible to screen for artificial binding partner, such as antigen-binding fragment (Fab), Nanobody (Nb) or a Monobody (Mb) [183].

Yet, the binding partner could induce conformational change of the interested protein. This may be beneficial for SPA, e.g. if the protein becomes more stable or is locked into certain conformation which means it is less dynamic. It is also possible to generate the preferred state by adding inhibitors or ligands to the protein, which makes the protein more stable and homogeneous.

4.1.2 Variables considering vitrification

Vitrification in cryoEM is achieved by using plunge-freezing with liquid ethane as described above [210]. Multiple rounds of sample application and blotting can be performed before plunge-freezing to increase the protein density on grid [211]. Since the liquid surrounding the protein sample scatters electrons as well, it generates background noise, thin ice is generally preferred to improve the signal-to-noise ratio [210].

The plasma during glow-discharging grids deposits charges on the grids, making the grids less hydrophobilic [212]. The amount of charge will change the liquid behaviour and influence particle distribution [213]. The blotting conditions (blotting time and force) are different for each protein sample as the sample concentration and buffer composition differ from each other, which changes viscosity of the solution [214], [215]. From these parameters empirical optimisation is necessary.

New methods have been developed as an alternative to blotting, such as, spraying (Surface Acoustic Waves [216] and polydimethylsiloxane-based sprayer [217]), inkjet dispensing (Spotiton [218] and Chameleon [214]), microcapillary cryoWriter [219] and contact pin printing VitroJet [220].

4.1.3 Grid choice

The most two common grid materials are copper and gold. Gold grids reduce the specimen motion during cryoEM imaging [221] and result in better data. The mesh size ranges usually from 200 to 400 mesh (Fig 11 is an example of copper gird with 200 mesh). The larger the mesh size the smaller the distance between metal bar. This provides more support to the film, which minimizes the damage to the support film caused by handling. If a support for the sample is needed, e.g. because of low sample concentration carbon films are avoided because they contribute substantially to the background signal. Graphene oxide could be an alternative to reduce the background signal if one collects data on a continuous film [222].

4.1.4 Orientation bias

Orientation bias means that protein particles adopt preferred orientation on the grid, resulting in 2D images that do not capture all possible particle views. This negatively impacts the cryoEM 3D maps. One of the major reasons for orientation bias is protein particle aggregation at the air-water interface and cause preferred orientation [223].

There are several strategies to overcome orientation bias: adding detergent at low concentrations (such as, Fluorinated Fos-Choline 8, 3-([3-Cholamidopropyl]dimethylammonio)-2-hydroxy-1-propanesulfonate) [134], [224]; collect data using a solid support layer over holes [213] and collect data with a tilted stage [225].

4.2 Image correction

The images generated in an electron microscope are collected with various defects, which need to be corrected to generate a true representation of the 3D object with a high resolution.

4.2.1 Motion correction

While imaging objects in an electron microscope, the sample does not stay still. The movement of the stage and vibration of the microscope can cause motion of the whole grid, which is referred to as stage drift [226], [227]. When electrons pass through the sample, they cause beam-induced ice deformation. The ice becomes bent in the grid holes, causing the movement of each particle in the sample (Fig. 12) [228]. The movement is three-dimensional, and each position moves differently (anisotropic). All this causes blurring in the final image.

In addition, the electrons cause radiation damage to the sample, which leads to the loss of high-resolution features over time [229]. Instead of taking a single long-time exposure, cameras/detectors capture images as multi-frame movies [230], [231]. In this way, high spatial frequencies would be recorded in the first few frames [231] and beam induced motion can be corrected, known as motion correction [232].

During motion correction each frame is aligned with respect to the preceding and following frame(s). Additionally, the high-frequency signals from the later frames is down-weighted when the images of a corrected movie are averaged to reduce noise [233].

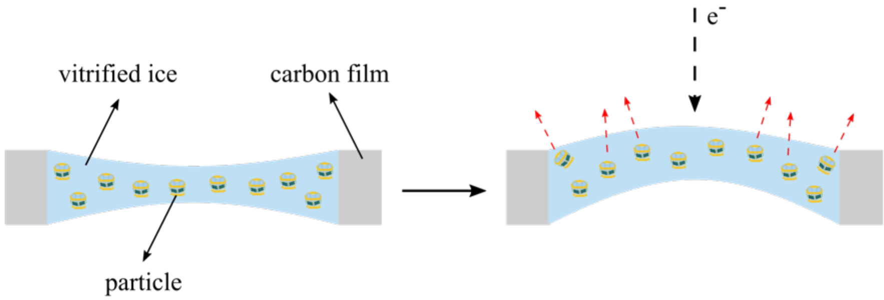

Figure 12. Schematic representation of beam-induced ice deformation. When the electron beam reaches the grid, it causes deformation of the vitreous ice layer.

4.2.2 CTF estimation

The point spread function (PSF) describes, in real space, how the true particle is altered into the final image in cryoEM [234]. The contrast transfer function (CTF) is the fourier transform of the PSF [235]. CTF describes how contrast is generated by microscope imperfections (spherical aberration), electron absorption (amplitude contrast) and defocus dependent phase contrast [236]–[238].

If we observe particles at perfect focus, particle contrast is very weak due to the weak phase contrast. Therefore, imaging is performed in under-defocus conditions to enhance the contrast [239], [240]. In addition, since the sample is not perfectly flat, there is uneven defocus across the field of view [241]. These factors cause the final image to be distorted.

The CTF can be estimated by performing a Fourier transform on the cryoEM image and then numerically fit the oscillating contrast pattern (thon rings) to the equation of the CTF [239]. From the CTF fit, we can estimate the precise defocus and astigmatism for each micrograph. Therefore, we need to perform CTF estimation for every micrograph and later correct these distortions to obtain an accurate structure [242].

The correlation of the estimated CTF with the experimental Thon rings also provides an estimate for the overall resolution of the micrograph [242].

4.3 Particle selection and curation

After image correction, the micrograph is ready for identifying and extracting images of the protein, also known as particle picking. There are different methods to identify particles. The most traditional way is to pick particles manually. This is not feasible for large datasets. However, the results of manual picks, can be used to generate templates for template picking (cross correlation between template and micrograph) or train deep neural network picking programs (such as such as, topaz, crYOLO, DRPnet, APPLE) to improve the picking results and to collect data for large datasets [243]–[246].

The identified protein images are extracted in a box with the size determined based on the particle size. Usually, 1.5 or 2 times larger than the particle, because the CTF/Fourier information extends a couple of pixels beyond the visible particle [247], [248]. Using a box too small would be the same as applying a low pass filter. The particles can be down sampled to increase the speed of data processing at the cost of resolution.

4.4 2D classification

During 2D classification, particles are aligned by means of rotation and translation with respect to each other [249]. Maximum likelihood approaches are frequently used to achieve this [250]. Here each particle is assigned a pose probability in relationship to a reference. Based on these estimated poses a new reference will be generated. This process is repeated. As a result, particles with similar shapes are grouped into the same class [251]. The advantage of the maximum likelihood approach is that the particles are not hard classified [252]. This reduces the chance of carrying over wrongly assigned particles through each iteration. This happens in early stages of the classification [253], [254].

The class average is important to improve the signal-to-noise ratio by reducing random noise. The resulting averages can provide information about composition, shape, assembly state and secondary structure elements. For curation, class averages are useful for identifying and discarding non-particle or 'junk' classes. This method can efficiently eliminate unrelated particle images [255]. Additionally, class averages can help distinguish and separate classes representing different proteins [256].

4.5 Ab-Initio reconstruction

The particles are 2D projections of the 3D volume, but the angle and shift (aka pose) between the 2D projections and the 3D structure are unknown. The goal of the 3D reconstruction is to determine the projection poses for each particle [257]. To achieve this, an initial reference volume is typically required, and the projection angles are refined iteratively. However, using an initial reference volume can introduce model bias and is not suitable for unknown proteins [258].

Ab-Initio reconstruction (CryoSparc) or De novo 3D model generation (Relion) is a method that creates a randomly generated 3D volume without using an user-provided reference model, thereby reducing the risk of model bias [254], [259]. The principle behind this reconstruction is once again maximum likelihood but adding another dimension for the estimation of the poses. Similar to 2D classification, multiple 3D volumes/maps can be generated from one particle set. This approach not only identifies volumes with distinct features. As a result, this approach provides the possibility to removing junk particles in addition to 2D classification.

4.6 3D refinement

Once an initial 3D volume has been reconstructed from a homogeneous dataset, 3D refinement is performed to further improve the alignment of individual particles. This process iteratively optimizes orientation and shift parameters (poses) by with finer sampling, to achieve higher-resolution maps [260], [261].

To avoid overfitting (treat noise as real structural signal therefore correlating it to higher resolution), the Fourier shell correlation (FSC) is calculated in the gold-standard way to estimate the resolution . To perform this, the dataset is randomly split into halves and refined independently. The FSC is calculated between the two volumes in fourier space to quantify the similarity between the two, independently generated volumes [262], [263]. A high FSC value means strong agreement between the reconstructions at any given resolution. Any correlation in the FSC curve drops below a threshold value of 0.143 is considered random and therefore acts as an indicator for the resolution of the reconstruction [262]. However, the actual threshold is still debated in the field [264].

4.7 Conformational variability

As mentioned above, *ab-initio* reconstruction can identify distinct maps. Heterogeneous refinement is usually performed afterward to reassign particles to different volumes generated from the *ab-initio* results and refine these [265]. This allows for the detection of subtle differences between structures that may not be apparent at low resolutions.

3D classification and 3D variability analysis (3DVA) are two additional methods used to identify heterogeneity (such as conformational changes) within the sample [266]. Those two function in CryoSparc can be performed at various resolutions to focus on structural changes at different levels of detail. Since the variance is negatively influenced by noise, it is important to test masks. This is particularly true for the transmembrane region, due to the noise of the unstructured detergent micelle or lipids. The difference between 3D variability analysis and 3D classification is, 3D classification assuming a limited number of rigid conformations, but 3DVA models a continuous family of 3D structures. This allows it to explore both discrete and continuous motions within the sample [266].

4.8 Post-processing

The downweighing of contrast at high frequencies of cryoEM 3D maps due to the envelope function of the microscope, makes it difficult to interpret the density. Therefore, post-processing tools like sharpening methods (using different contrast restoration algorithms) can employed to improve its interpretability.

The most common approach is global sharpening with a single B-factor, such as Relion and CryoSparc. However, the approach will boost noise if there is no information at a given resolution of the map [267].

Local sharpening algorithms have been proposed to only manipulate the B factor at the maximum local resolution in cryoEM maps, such as LocScale, LocalDeblur and LocSpiral [267]–[270]. All of them need a priori information about the target map, namely the independently reconstructed maps ('Half-Maps').

DeepEMhancer is a fully automatic deep learning-based local sharpening algorithms which do not need priori information and instead rely on training parameters derived from all models and maps in the PDB database [271].

5 Present investigation

PANX1 is an membrane channel that controls the release of signalling molecule ATP. The activation mechanism of PANX1 that lead to ATP release is not full understood. Therefore, we aim to investigate the machinsm of PANX1 activation by using cryoEM to study the structure and electrophoysiology to study the function.

Besides using cryoEM to study a specific protein in homogenous sample, we also would like to develop a workflow for identifying and determining the structures of membrane proteins in a heterogeneous sample; without prior knowledge of the protein sequence or a model. Meanwhile, we are also exploring another membrane protein, SMCT1 transporter and conducting prelimily studies to investigate its interaction partner PDZ1.

5.1 Paper I: Structural basis of ATP release and ion selectivity in Pannexin1 channels

ATP is the primary energy source of cells, in addition, it also plays important role as a signalling molecule. Pannexin 1 (PANX1) is one of the key channel responsible for ATP release. Aberrant Panx1 activity has been associated with several neurological disorders including seizure, stroke, migraine headache and chronic pain. Previous studies suggest there are two ways to activate Panx1 release ATP, either by irreversible caspase-mediated cleavage or reversible phosphorylation. In this study, I aimed to determine whether phosphorylation acts as a reversible switch for PANX1 activation, how the structure changes during activation by phosphorylation.

To confirm that phosphorylation does activate PANX1, TEVC was employed to measure the electrophysiology of mouse-PANX1-expressing Xenopus oocytes while injecting them with a constitutively active form of SRC (v-SRC is a kinase). Outward currents were only observed when a single v-SRC injection but not with albumin injection (as control) or v-SRC with without PANX1. This confirmed the theory phosphorylation can active PANX1.

To further investigate which sites are phosphorylated by SRC, mass spectrometry were performed on both dephosphorylated and re-phosphorylated Panx1. We identified four potential phosphorylation site (Y10, S181, Y308, S406). Electrophysiological recordings in Xenopus oocytes and ATP release assays with phosphomimetic and phosphosuppressive mutants (Y10E, Y198E, Y308E, Y198F) revealed Y308E mutant converts Panx1 into a constitutively open channel. It suggests phosphorylation at Y308 may serve as a potential switch.

CryoEM structure of SRC phosphorylated PANX1 (PanxSRC) were obtained with a resolution of 3.56Å. Movement of the transmembrane domain were observed during 3DVA analysis. The structure moving between narrow and wide confromation with N-terminal relaxed and ordered, respecitvely. The same phonomenon was also observed with R75A mutant.

CryoEM structure of the Y308E mutant showed that the channel adopts a wide conformation with N-terminal ordered. Electrophysiology data also confirmed its permeability to ATP. Further conformational variability analysis (both 3DVA and 3D classification), shows there is no flexibility in transmembrane region. However, there is twist moving in the intracellular region, which is the worse resolved part of the structure.

In conclusion, our MS and electrophysiology data confirmed PANX1 is not only phosphorylated by SRC, but also that the phosphorylation activates it. CryoEM data shows, suggest that the transmembrane region of both PanxSRC and R75A mutant is flexible and moving between narrow and wide conformation with different arrangement of N-terminal end. Y308 mutant were only observed with wide conformation and with ATP permeability. This suggests Y308 is a phosphorylation site that may switches Panx1 into wide conformation, enabling ATP release.

5.2 Paper II: *In silico* classification and identification co-purified protein complexes yield new structures and multiple MSP assembly states

Traditional methods, like X-ray and NMR require a homogeneous and stable sample. Single-particle analysis (SPA), on the other hand, enables high-resolution reconstruction of proteins in a heterogeneous sample. 2D and 3D classification can be used to identify and determine structures of multiple proteins in one heterogeneous sample. In previous workflows, mass spectrometry (MS) was needed to identify proteins. Here we present a modified workflow for identifying and determining the structures of membrane proteins in a heterogeneous sample; without prior knowledge of the protein sequence or a model.

We enriched *E. coli* membrane proteins by immobilized metal (nickel) affinity chromatography (IMAC) and reconstituted the proteins into MSP2N2 nanodiscs. The mixture was then fractionated by SEC and concentrated for SPA and MS for independent verification. We sorted protein populations by 2D classification. After ab-initio reconstruction and refinement in the CryoSparc software, we were able to generate three different maps.

To identify proteins, we used ModelAngelo to build models with the maps. Since the identity of the proteins was not known we only supplied the entire *E. coli* proteome to perform an HMMER search with the unsupervised built model fragments. In this way we identified and resolved three proteins: the cytochrome bo3 ubiquinol oxidase (BO3, 2.72 Å), the multidrug efflux pump subunit AcrB (AcrB, 3.27 Å), and the new undecaprenyl-phosphate 4-deoxy-4-formamido-L-arabinose transferase (ArnC). Independent MS analysis identified the three proteins in our sample.

Notably, MSP2N2 in nanodiscs, assembled differently (dimeter, number of helical rungs, shape) around these three proteins. We also found membrane protein sidechains are close to the predicted MSP2N2 density suggesting that embedded proteins actively shape nanodisc assembly.

In summary, we present a streamlined workflow for recognizing and modelling membrane proteins in a heterogenous sample. The workflow delivered a new structure (ArnC) and provides evidence that nanodisc architecture is not a passive but depends on specific protein–scaffold interactions.

5.3 Paper III: SMCT1 has a low affinity to PDZ domain containing 1 protein

Sodium-coupled monocarboxylate transporter 1 (SMCT1) is a membrane transporter abundantly expressed human body such as, colon, kidney, thyroid, brain. It transports monocarboxylic acids with little specificity into cells. A Study shows that two PDZ domains (PDZ1 and PDZ3) of the scaffolding protein PDZ Domain Containing 1 (PDZK1) interact with SMCT1 and increases its transport activity. This study aims to investigate whether the affinity between SMCT1 and PDZ1/3 is physiologically meaningful.

We first performed pull-down assays with SMCT1-GFP to catch PDZ1-MBP and PDZ3-MBP in solution. SDS-PAGE confirmed binding between SMCT1-GFP with PDZ1-MBP (Maltose binding protein) and PDZ3- MBP.

To quantify the affinity between these two proteins, we employed surface plasmon resonance (SPR). To simplify the system we synthesized a PEPTIDE containing the PDZ motif from SMCT1. We first immobilize the peptide on SPR chip, but no binding between PEPTIDE and either PDZ1-MBP or PDZ3-MBP construct was observed. We reversed the mobile and stationary component to rule out the possibility that immobilization the obstructed the PDZ motif. This time the sensorgram showed that the PEPTIDE bound to both PDZ1-MBP and PDZ3-MBP, with rapid association and dissociation rate and the equilibrium dissociation constant (KD) could not be calculated.

We used microscale thermophoresis (MST) to measure the affinity between full-length SMCT1-GFP and PDZ1 and PDZ3-MBP, to see if there is more to the binding than the isolated peptide. But we never reached saturation and the KD was estimated in the mid μM range.

In summary, all experiments including pull-down assays, SPR and MST shows binding between PDZ1 /3 and SMCT1 (or PEPTIDE from SMCT1). Yet, the affinity is weak. We therefore suggest that the interaction between PDZ1/3 and SMCT1 is likely physiologically irrelevant, except in special cases, where PDZK1 is locally enriched at membrane.

5.4 Conclusion and future perspective

Cryo-EM SPA is a powerful technique. It allows us to visualize small proteins such as SMCT1, when in a homogeneous protein prepation. Or we can study heterogeneous samples, whether it is protein flexibility (conformational heterogenous), as in PANX1, or a mixture of proteins (compositional heterogeneous) (paper II). Together with biophysical, functional methods like electrophysiology, SPR, and MST, we can comprehensively correlate structural information with functional properties, revealing the underlying molecular mechanisms.

In the future, the PANX1 project should be continued by including the WT. It will be important to confirm whether WT PANX1 also has flexibility in the transmembrane region. In addition, the R217H mutation, a natural PANX1 variant with significantly reduced activity, could be an interesting candidate.

The modified workflow presented in paper II could be applied to study proteins that are pulled out of a lysate with a common binding motif, say the PDZ binding motif. Specific affibodies or nanobodies can be raised to bind strongly to specific PDZ binding motifs and used to purify proteins containing PDZ binding motifs from cell mixtures.

Acknowledgement

I would like to thank all the organizations that have supported my research. Special thanks to the China Scholarship Council, which gave me the opportunity to begin my PhD here at KTH. Many thanks to the Department of Biomedical Engineering and Health Systems, the Department of Protein Science at KTH, as well as the Biosciences and Nutrition Unit and the Clinical Research Center at KI for supporting my studies. I am also grateful to all the people who have helped me along the way and made this journey possible.

First, I would like to express my deepest gratitude to my main supervisor, **Carsten**, for his continuous support and guidance. Carsten has always been so patient and kind to me. His passion and optimism for science have truly inspired me and helped me persevere even when experiments were difficult. I would also like to thank my co-supervisors, **Philip** and **Rebecca**, for their invaluable help and support during my studies.

I am also grateful to all the members of our research group. Although our division was enventually disbanded, it was a great honor to work with you all. Thank you, **Caroline** and **Pasi**, for all the wisdom you shared during group meetings. Thank you, **Abhi** and **Tales**, for guiding me through the lab when I first started. And thank you, **Xueying** and **Zuoneng**, for your friendship throughout the PhD years, even after you continued on to the next exciting chapters of your careers.

I would like to thank everyone at the Department of Biomedical Engineering and Health Systems. **Fangyuan**, **Hongjian**, **Huangqi** and **Zhouzhou**, it has been such a joy to have you around.

Many thanks as well to my colleagues at the Biosciences and Nutrition Unit and Clinical Research Center. Thank you, **Feifei**, **Herui**, **Kathrin**, and **Yawen**, who working so closely with me and for all the help you have provided throughout my research.

I would also like to thank everyone at the Department of Protein Science. I joined this department near the end of my PhD, and I am so grateful for how inspiring and friendly this period has been. Thank you to my office mates **Ábel**, **Charlie**, **Oscar**, **Gustav** and **Marit** for all the great "streching" times we shared. It was a pleasure to share the office with you. I would also like to thank **Jacob** and **Kristina** for their valuable help with the peptide synthesis. It was a great pleasure working with you. Thanks also to all the PIs in the department. A special thanks to **Sofia**, for welcoming me to the department, and to **Per-Åke**, for sharing his insights on my research. His advice were incredibly helpful and informative.

I would also like to thank all my climbing buddies: **Alice**, **Jingru**, **Malin**, **Morong**, **Shengyuan** and **Tailang**. Climbing with you was so much fun and helped me forget all the stress I had during my research.

Last but not least, I would like to thank my family and friends. To the person who means the most to me, my husband **Haozhong**. Thank you for your endless support and love. And to my parents, for your unconditional love and constant encouragement throughout my life. Finally, to my dear friends **Jie**, **Luyao**, **Ruonan**, **Shenyang**, **shu-Chieh**, **Yizhou** and **Yuyang** thank you for accompanying me through this incredible journey.

References

[1] G. M. Cooper, *The Cell: A Molecular Approach*, 2nd editio. Sunderland (MA): Sinauer Associates, 2000.

[2] J. Lombard, “Once upon a time the cell membranes: 175 years of cell boundary research,” *Biol. Direct*, vol. 9, no. 1, pp. 1–35, Dec. 2014.

[3] M. S. Almén, K. J. V. Nordström, R. Fredriksson, and H. B. Schiöth, “Mapping the human membrane proteome: A majority of the human membrane proteins can be classified according to function and evolutionary origin,” *BMC Biol.*, vol. 7, p. 50, 2009.

[4] N. Soni, B. V. K. Reddy, and P. Kumar, “GLT-1 transporter: An effective pharmacological target for various neurological disorders,” *Pharmacol. Biochem. Behav.*, vol. 127, pp. 70–81, 2014.

[5] R. J. Harvey and B. K. Yee, “Glycine transporters as novel therapeutic targets in schizophrenia, alcohol dependence and pain,” *Nat. Rev. Drug Discov.*, vol. 12, no. 11, pp. 866–885, 2013.

[6] N. Gupta, P. M. Martin, P. D. Prasad, and V. Ganapathy, “SLC5A8 (SMCT1)-mediated transport of butyrate forms the basis for the tumor suppressive function of the transporter,” *Life Sci.*, vol. 78, no. 21, pp. 2419–2425, 2006.

[7] K. C. Chou and H. Bin Shen, “MemType-2L: A Web server for predicting membrane proteins and their types by incorporating evolution information through Pse-PSSM,” *Biochem. Biophys. Res. Commun.*, vol. 360, no. 2, pp. 339–345, Aug. 2007.

[8] P. L. Yeagle, “Chapter 10 – Membrane proteins,” in *The*

Membranes of Cells, 3rd ed., P. L. Yeagle, Ed. Academic Press, 2016, pp. 219–268.

[9] N. Yan, "A Glimpse of Membrane Transport through Structures—Advances in the Structural Biology of the GLUT Glucose Transporters," *J. Mol. Biol.*, vol. 429, no. 17, pp. 2710–2725, 2017.

[10] S. Sowlati-Hashjin, A. Gandhi, and M. Garton, "Dawn of a New Era for Membrane Protein Design," *BioDesign Res.*, vol. 2022, p. 9791435, 2022.

[11] B. Alberts, D. Morgan, A. Johnson, J. Lewis, and M. Raff, *Molecular Biology of the Cell*, 4th editio. New York: Garland Science, 2002.

[12] S. Srivastava *et al.*, "Identification of the multivalent PDZ protein PDZK1 as a binding partner of sodium–coupled monocarboxylate transporter SMCT1 (SLC5A8) and SMCT2 (SLC5A12)," *J. Physiol. Sci.*, vol. 69, no. 2, pp. 399–408, 2019.

[13] R. P. Piprek, M. Kloc, P. Mizia, and J. Z. Kubiak, "The central role of cadherins in gonad development, reproduction, and fertility," *Int. J. Mol. Sci.*, vol. 21, no. 21, 2020.

[14] K. U. Ashraf *et al.*, "Structural basis of undecaprenyl phosphate glycosylation leading to polymyxin resistance in Gram-negative bacteria," pp. 1–41, 2025.

[15] E. Gopal *et al.*, "Transport of nicotinate and structurally related compounds by human SMCT1 (SLC5A8) and its relevance to drug transport in the mammalian intestinal tract," *Pharm. Res.*, vol. 24, no. 3, pp. 575–584, 2007.

[16] E. Rivas-Yáñez *et al.*, "P2x7 receptor at the crossroads of t cell fate," *Int. J. Mol. Sci.*, vol. 21, no. 14, pp. 1–22, 2020.

[17] M. C. Good, J. G. Zalatan, and W. A. Lim, "Scaffold Proteins:

Hubs for Controlling the Flow of Cellular Information.”

[18] E. Kim and M. Sheng, “PDZ domain proteins of synapses,” *Nat. Rev. Neurosci.*, vol. 5, no. 10, pp. 771–781, 2004.

[19] H. Tochio, Q. Zhang, P. Mandal, M. Li, and M. Zhang, “Solution structure of the extended neuronal nitric oxide synthase PDZ domain complexed with an associated peptide,” *Nat. Struct. Biol.*, vol. 6, no. 5, pp. 417–421, 1999.

[20] Y. Otsuka *et al.*, “Sodium-coupled monocarboxylate transporter 1 interacts with the RING finger- and PDZ domain-containing protein PDZRN3,” *J. Physiol. Sci.*, vol. 69, no. 4, pp. 635–642, 2019.

[21] G. F. Weber, M. A. Bjerke, and D. W. DeSimone, “Integrins and cadherins join forces to form adhesive networks,” *J. Cell Sci.*, vol. 124, no. 8, pp. 1183–1193, Apr. 2011.

[22] Y. Rikitake and Y. Takai, “Interactions of the cell adhesion molecule nectin with transmembrane and peripheral membrane proteins for pleiotropic functions,” *Cellular and Molecular Life Sciences*, vol. 65, no. 2. pp. 253–263, Jan-2008.

[23] S. Brady, S. Brady, G. Siegel, G. Siegel, R. W. Albers, and D. L. Price, Eds., *Basic Neurochemistry: Molecular, Cellular and Medical Aspects*, 6th editio. Philadelphia: Lippincott-Raven, 1999.

[24] M. Takeichi, “Cadherin Cell Adhesion Receptors as a Morphogenetic Regulator,” *Science (80-.).*, vol. 251, no. 5000, pp. 1451–1455, 1991.

[25] S. Müller-Loennies, L. Brade, and H. Brade, “Neutralizing and cross-reactive antibodies against enterobacterial lipopolysaccharide,” *Int. J. Med. Microbiol.*, vol. 297, no. 5, pp. 321–340, Sep. 2007.

[26] B. Khalil, E. J. Miller, and S. L. Lappin, *Physiology, Cellular Receptors*. Treasure Island (FL): StatPearls Publishing.

[27] P. A. Insel *et al.*, "GPCRomics: An Approach to Discover GPCR Drug Targets," *Trends Pharmacol. Sci.*, vol. 40, no. 6, pp. 378–387, Jun. 2019.

[28] S. Liu, P. J. Anderson, S. Rajagopal, R. J. Lefkowitz, and H. A. Rockman, "G Protein-Coupled Receptors: A Century of Research and Discovery," *Circ. Res.*, vol. 135, no. 1, pp. 174–197, Jun. 2024.

[29] L. Cheng *et al.*, "Structure, function and drug discovery of GPCR signaling," *Mol. Biomed.*, vol. 4, no. 1, p. 46, Dec. 2023.

[30] E. Li and K. Hristova, "Role of Receptor Tyrosine Kinase Transmembrane Domains in Cell Signaling and Human Pathologies†," *Biochemistry*, vol. 45, no. 20, pp. 6241–6251, May 2006.

[31] S. Alexander, A. Mathie, and J. Peters, "Ion Channels," *Br. J. Pharmacol.*, vol. 164, no. Suppl 1, p. S137, Nov. 2011.

[32] Q. Huang, W. Zhu, X. Gao, X. Liu, Z. Zhang, and B. Xing, "Nanoparticles-mediated ion channels manipulation: From their membrane interactions to bioapplications," *Adv. Drug Deliv. Rev.*, vol. 195, p. 114763, Apr. 2023.

[33] B. S. Barker, G. T. Young, C. H. Soubrane, G. J. Stephens, E. B. Stevens, and M. K. Patel, "Ion Channels," *Conn's Transl. Neurosci.*, pp. 11–43, Jan. 2017.

[34] J. Syrjanen, K. Michalski, T. Kawate, and H. Furukawa, "On the molecular nature of large-pore channels," *J. Mol. Biol.*, vol. 433, no. 17, p. 166994, Aug. 2021.

[35] J. E. Contreras, J. C. Sáez, F. F. Bukauskas, and M. V. L. Bennett, "Gating and regulation of connexin 43 (Cx43)

hemichannels," *Proc. Natl. Acad. Sci. U. S. A.*, vol. 100, no. 20, p. 11388, Sep. 2003.

[36] E. B. Trexler, F. F. Bukauskas, M. V. L. Bennett, T. A. Bargiello, and V. K. Verselis, "Rapid and Direct Effects of pH on Connexins Revealed by the Connexin46 Hemichannel Preparation," *J. Gen. Physiol.*, vol. 113, no. 5, p. 721, May 1999.

[37] J. M. Gómez-Hernández, M. De Miguel, B. Larrosa, D. González, and L. C. Barrio, "Molecular basis of calcium regulation in connexin-32 hemichannels," *Proc. Natl. Acad. Sci. U. S. A.*, vol. 100, no. 26, pp. 16030–16035, Dec. 2003.

[38] G. Söhl and K. Willecke, "An update on connexin genes and their nomenclature in mouse and man," *Cell Commun. Adhes.*, vol. 10, no. 4–6, pp. 173–180, 2003.

[39] S. A. Lucaciu, S. E. Leighton, A. Hauser, R. Yee, and D. W. Laird, "Diversity in connexin biology," *J. Biol. Chem.*, vol. 299, no. 11, p. 105263, Nov. 2023.

[40] W. Lopez, J. Ramachandran, A. Alsamarah, Y. Luo, A. L. Harris, and J. E. Contreras, "Mechanism of gating by calcium in connexin hemichannels," *Proc. Natl. Acad. Sci. U. S. A.*, vol. 113, no. 49, pp. E7986–E7995, Dec. 2016.

[41] B. C. Bennett *et al.*, "An electrostatic mechanism for Ca2+-mediated regulation of gap junction channels," *Nat. Commun.*, vol. 7, Jan. 2016.

[42] A. K. Khan *et al.*, "A Steric 'Ball-and-Chain' Mechanism for pH-Mediated Regulation of Gap Junction Channels," *Cell Rep.*, vol. 31, no. 3, p. 107482, Apr. 2020.

[43] A. Taruno, "ATP Release Channels," *Int. J. Mol. Sci.*, vol. 19, no. 3, p. 808, Mar. 2018.

[44] G. E. Sosinsky and B. J. Nicholson, "Structural organization

of gap junction channels,” *Biochim. Biophys. Acta - Biomembr.*, vol. 1711, no. 2, pp. 99–125, Jun. 2005.

[45] H. Sadamoto, H. Takahashi, S. Kobayashi, H. Kondoh, and H. Tokumaru, “Identification and classification of innexin gene transcripts in the central nervous system of the terrestrial slug Limax valentianus,” *bioRxiv*, p. 2020.12.21.423878, Dec. 2020.

[46] Z. Ruan, I. J. Orozco, J. Du, and W. Lü, “Structures of human pannexin 1 reveal ion pathways and mechanism of gating,” *Nature*, vol. 584, no. 7822, pp. 646–651, 2020.

[47] T. Yamada, P. Bisignano, E. Karakas, and J. S. Denton, “A conserved mechanism of LRRC8 channel inhibition by two structurally distinct drugs,” *Commun. Biol. 2025 81*, vol. 8, no. 1, pp. 1–13, Oct. 2025.

[48] J. L. Syrjänen, M. Epstein, R. Gómez, and H. Furukawa, “Structure of human CALHM1 reveals key locations for channel regulation and blockade by ruthenium red,” *Nat. Commun. 2023 141*, vol. 14, no. 1, pp. 1–13, Jun. 2023.

[49] Z. Huang *et al.*, “From purines to purinergic signalling: molecular functions and human diseases,” *Signal Transduct. Target. Ther. 2021 61*, vol. 6, no. 1, pp. 1–20, Apr. 2021.

[50] G. Burnstock, “Historical review: ATP as a neurotransmitter,” *Trends Pharmacol. Sci.*, vol. 27, no. 3, pp. 166–176, Mar. 2006.

[51] M. P. Abbracchio, G. Burnstock, A. Verkhratsky, and H. Zimmermann, “Purinergic signalling in the nervous system: an overview,” *Trends Neurosci.*, vol. 32, no. 1, pp. 19–29, Jan. 2009.

[52] A. Baranova *et al.*, “The mammalian pannexin family is homologous to the invertebrate innexin gap junction proteins,” *Genomics*, vol. 83, no. 4, pp. 706–716, Apr. 2004.

[53] A. K. Yeung, C. S. Patil, and M. F. Jackson, “Pannexin-1 in the CNS: Emerging concepts in health and disease,” *J. Neurochem.*, vol. 154, no. 5, pp. 468–485, 2020.

[54] F. J. Bravo *et al.*, “The impact of Panx1 on inflammation, immunity, and cancer: a comprehensive review,” *Front. Med.*, vol. 12, p. 1572418, 2025.

[55] D. Nouri-Nejad *et al.*, “Pannexin 1 mutation found in melanoma tumor reduces phosphorylation, glycosylation, and trafficking of the channel-forming protein,” *Mol. Biol. Cell*, vol. 32, no. 5, pp. 376–390, 2021.

[56] K. E. Navis, C. Y. Fan, T. Trang, R. J. Thompson, and D. J. Derksen, “Pannexin 1 Channels as a Therapeutic Target: Structure, Inhibition, and Outlook,” *ACS Chem. Neurosci.*, vol. 11, no. 15, pp. 2163–2172, 2020.

[57] M. Koval, W. J. Schug, and B. E. Isakson, “Pharmacology of pannexin channels,” *Curr. Opin. Pharmacol.*, vol. 69, p. 102359, 2023.

[58] W. Silverman, S. Locovei, and G. Dahl, “Probenecid, a gout remedy, inhibits pannexin 1 channels,” *Am. J. Physiol. Physiol.*, vol. 295, no. 3, pp. C761–C767, Sep. 2008.

[59] E. Scemes and J. Velíšková, “Exciting and not so exciting roles of pannexins,” *Neurosci. Lett.*, vol. 695, pp. 25–31, Mar. 2019.

[60] K. Michalski and T. Kawate, “Carbenoxolone inhibits Pannexin1 channels through interactions in the first extracellular loop,” *J. Gen. Physiol.*, vol. 147, no. 2, pp. 165–174, Feb. 2016.

[61] R. Qu, L. Dong, J. Zhang, X. Yu, L. Wang, and S. Zhu, “Cryo-EM structure of human heptameric Pannexin 1 channel,” *Cell Res.*, vol. 30, no. 5, pp. 446–448, 2020.

[62] L. Mou *et al.*, “Structural basis for gating mechanism of Pannexin 1 channel,” *Cell Res.*, vol. 30, no. 5, pp. 452–454, 2020.

[63] Q. Jin *et al.*, “Cryo-EM structures of human pannexin 1 channel,” *Cell Res.*, vol. 30, no. 5, pp. 449–451, 2020.

[64] Z. Deng *et al.*, “Cryo-EM structures of the ATP release channel pannexin 1,” *Nat. Struct. Mol. Biol.*, vol. 27, no. 4, pp. 373–381, 2020.

[65] K. Michalski, J. L. Syrjanen, E. Henze, J. Kumpf, H. Furukawa, and T. Kawate, “The Cryo-EM structure of a pannexin 1 reveals unique motifs for ion selection and inhibition,” *Elife*, vol. 9, pp. 1–14, 2020.

[66] N. Hussain *et al.*, “Cryo-EM structures of pannexin 1 and 3 reveal differences among pannexin isoforms,” no. October 2022, 2024.

[67] Z. He *et al.*, “Structural and functional analysis of human pannexin 2 channel,” *Nat. Commun. 2023 141*, vol. 14, no. 1, pp. 1–10, Mar. 2023.

[68] F. B. Chekeni *et al.*, “Pannexin 1 channels mediate ‘find-me’ signal release and membrane permeability during apoptosis,” *Nature*, vol. 467, no. 7317, pp. 863–867, 2010.

[69] J. K. Sandilos *et al.*, “Pannexin 1, an ATP release channel, is activated by caspase cleavage of its pore-associated C-terminal autoinhibitory region,” *J. Biol. Chem.*, vol. 287, no. 14, pp. 11303–11311, 2012.

[70] C. Mim, G. Perkins, and G. Dahl, “Structure versus function: Are new conformations of pannexin 1 yet to be resolved?,” *J. Gen. Physiol.*, vol. 153, no. 5, pp. 1–17, 2021.

[71] J. Wang, C. Ambrosi, F. Qiu, D. G. Jackson, G. Sosinsky, and G. Dahl, “The membrane protein Pannexin1 forms two open-

channel conformations depending on the mode of activation," *Sci. Signal.*, vol. 7, no. 335, Jul. 2014.

[72] G. Dahl, "The Pannexin1 membrane channel: distinct conformations and functions," *FEBS Lett.*, vol. 592, no. 19, pp. 3201–3209, Oct. 2018.

[73] L. Bao, S. Locovei, and G. Dahl, "Pannexin membrane channels are mechanosensitive conduits for ATP," *FEBS Lett.*, vol. 572, no. 1–3, pp. 65–68, 2004.

[74] S. Locovei, J. Wang, and G. Dahl, "Activation of pannexin 1 channels by ATP through P2Y receptors and by cytoplasmic calcium," *FEBS Lett.*, vol. 580, no. 1, pp. 239–244, Jan. 2006.

[75] W. R. Silverman *et al.*, "The Pannexin 1 Channel Activates the Inflammasome in Neurons and Astrocytes," *J. Biol. Chem.*, vol. 284, no. 27, pp. 18143–18151, Jul. 2009.

[76] E. Henze *et al.*, "ATP-release pannexin channels are gated by lysophospholipids," *Elife*, vol. 14, p. RP107067, May 2025.

[77] K. Yang, Z. Xiao, X. He, R. Weng, X. Zhao, and T. Sun, "Mechanisms of Pannexin 1 (PANX1) Channel Mechanosensitivity and Its Pathological Roles," *Int. J. Mol. Sci.*, vol. 23, no. 3, pp. 1–12, 2022.

[78] I. Martins *et al.*, "Molecular mechanisms of ATP secretion during immunogenic cell death," *Cell Death Differ.*, vol. 21, no. 1, p. 79, Jan. 2013.

[79] A. M. Navale and A. N. Paranjape, "Glucose transporters: physiological and pathological roles," *Biophys. Rev.*, vol. 8, no. 1, p. 5, Mar. 2016.

[80] R. Luis, "Mechanisms of Ion Transport Across Cell Membranes and Epithelia," *Seldin Giebisch's Kidney Physiol. Pathophysiol. 1-2*, pp. 35–56, Jan. 2008.

[81] N. Fischer and C. Kandt, “Porter domain opening and closing motions in the multi-drug efflux transporter AcrB,” *Biochim. Biophys. Acta - Biomembr.*, vol. 1828, no. 2, pp. 632–641, Feb. 2013.

[82] D. Drew and O. Boudker, “Shared Molecular Mechanisms of Membrane Transporters,” *Annu. Rev. Biochem.*, vol. 85, pp. 543–572, 2016.

[83] A. Yamashita, S. K. Singh, T. Kawate, Y. Jin, and E. Gouaux, “Crystal structure of a bacterial homologue of Na+/Cl --dependent neurotransmitter transporters,” *Nature*, vol. 437, no. 7056, pp. 215–223, Sep. 2005.

[84] C. Colas, P. M. U. Ung, and A. Schlessinger, “SLC transporters: structure, function, and drug discovery,” *Medchemcomm*, vol. 7, no. 6, pp. 1069–1081, Jun. 2016.

[85] A. P. Halestrap and N. T. Price, “The proton-linked monocarboxylate transporter (MCT) family: structure, function and regulation,” *Biochem. J.*, vol. 343, no. Pt 2, p. 281, Oct. 1999.

[86] K. Pierre and L. Pellerin, “Monocarboxylate transporters in the central nervous system: distribution, regulation and function,” *J. Neurochem.*, vol. 94, no. 1, pp. 1–14, Jul. 2005.

[87] M. K. Jha and B. M. Morrison, “Lactate Transporters Mediate Glia-Neuron Metabolic Crosstalk in Homeostasis and Disease,” *Front. Cell. Neurosci.*, vol. 14, no. September, pp. 1–11, 2020.

[88] V. Ganapathy *et al.*, “Sodium-coupled monocarboxylate transporters in normal tissues and in cancer,” *AAPS J.*, vol. 10, no. 1, pp. 193–199, 2008.

[89] P. A. Marks, R. A. Rifkind, V. M. Richon, R. Breslow, T. Miller, and W. K. Kelly, “Histone deacetylases and cancer: Causes and therapies,” *Nat. Rev. Cancer*, vol. 1, no. 3, pp.

194–202, 2001.

[90] A. L. Rodd, K. Ververis, and T. C. Karagiannis, “Current and Emerging Therapeutics for Cutaneous T-Cell Lymphoma: Histone Deacetylase Inhibitors,” *Lymphoma*, vol. 2012, no. 1, p. 290685, Jan. 2012.

[91] L. Han *et al.*, “Structure and mechanism of the SGLT family of glucose transporters,” *Nature*, vol. 601, no. 7892, pp. 274–279, 2022.

[92] A. Pandey, K. Shin, R. E. Patterson, X. Q. Liu, and J. K. Rainey, “Current strategies for protein production and purification enabling membrane protein structural biology,” *Biochem. Cell Biol.*, vol. 94, no. 6, pp. 507–527, 2016.

[93] A. Kuhn, H.-G. Koch, and R. E. Dalbey, “Targeting and Insertion of Membrane Proteins,” *EcoSal Plus*, vol. 7, no. 2, pp. 10.1128/ecosalplus.ESP-0012–2016, Dec. 2017.

[94] B. Krishnarjuna and A. Ramamoorthy, “Detergent-Free Isolation of Membrane Proteins and Strategies to Study Them in a Near-Native Membrane Environment,” *Biomolecules*, vol. 12, no. 8, p. 1076, Aug. 2022.

[95] M. Freigassner, H. Pichler, and A. Glieder, “Tuning microbial hosts for membrane protein production,” *Microb. Cell Fact.*, vol. 8, no. 1, pp. 1–22, Dec. 2009.

[96] E. P. Carpenter, K. Beis, A. D. Cameron, and S. Iwata, “Overcoming the challenges of membrane protein crystallography,” *Curr. Opin. Struct. Biol.*, vol. 18, no. 5, pp. 581–586, 2008.

[97] A. M. Seddon, P. Curnow, and P. J. Booth, “Membrane proteins, lipids and detergents: Not just a soap opera,” *Biochim. Biophys. Acta - Biomembr.*, vol. 1666, no. 1–2, pp. 105–117, 2004.

[98] F. Junge, B. Schneider, S. Reckel, D. Schwarz, V. Dötsch, and F. Bernhard, “Large-scale production of functional membrane proteins,” *Cell. Mol. Life Sci.*, vol. 65, no. 11, pp. 1729–1755, Jun. 2008.

[99] C. G. Tate, A. Engel, and G. Semenza, “Overexpression of mammalian integral membrane proteins for structural studies,” *FEBS Lett.*, vol. 504, no. 3, pp. 94–98, Aug. 2001.

[100] A. Kesidis *et al.*, “Expression of eukaryotic membrane proteins in eukaryotic and prokaryotic hosts,” *Methods*, vol. 180, pp. 3–18, Aug. 2020.

[101] F. Bernaudat *et al.*, “Heterologous Expression of Membrane Proteins: Choosing the Appropriate Host,” *PLoS One*, vol. 6, no. 12, p. e29191, Dec. 2011.

[102] S. K. Kwon, S. K. Kim, D. H. Lee, and J. F. Kim, “Comparative genomics and experimental evolution of Escherichia coli BL21(DE3) strains reveal the landscape of toxicity escape from membrane protein overproduction,” *Sci. Rep.*, vol. 5, no. 1, pp. 1–13, Nov. 2015.

[103] S. Wagner *et al.*, “Tuning Escherichia coli for membrane protein overexpression.,” *Proc. Natl. Acad. Sci. U. S. A.*, vol. 105, no. 38, pp. 14371–14376, 2008.

[104] G. L. Rosano and E. A. Ceccarelli, “Recombinant protein expression in Escherichia coli: Advances and challenges,” *Frontiers in Microbiology*, vol. 5, no. APR. 2014.

[105] D. L. Atroshenko, E. P. Sergeev, D. I. Golovina, and A. A. Pometun, “Additivities for Soluble Recombinant Protein Expression in Cytoplasm of Escherichia coli,” *Ferment. 2024, Vol. 10, Page 120*, vol. 10, no. 3, p. 120, Feb. 2024.

[106] N. Oganesyan, I. Ankoudinova, S. H. Kim, and R. Kim, “Effect of Osmotic Stress and Heat Shock in Recombinant Protein Overexpression and Crystallization,” *Protein Expr.*

Purif., vol. 52, no. 2, p. 280, Apr. 2006.

[107] T. S. Tillman *et al.*, “Functional Human α7 Nicotinic Acetylcholine Receptor (nAChR) Generated from Escherichia coli,” *J. Biol. Chem.*, vol. 291, no. 35, p. 18276, Aug. 2016.

[108] A. Deb *et al.*, “Bacterial expression, correct membrane targeting and functional folding of the HIV-1 membrane protein Vpu using a periplasmic signal peptide,” *PLoS One*, vol. 12, no. 2, p. e0172529, Feb. 2017.

[109] Y. He, K. Wang, and N. Yan, “The recombinant expression systems for structure determination of eukaryotic membrane proteins,” *Protein Cell*, vol. 5, no. 9, pp. 658–672, Sep. 2014.

[110] J. A. Lyons, A. Shahsavar, P. A. Paulsen, B. P. Pedersen, and P. Nissen, “Expression strategies for structural studies of eukaryotic membrane proteins,” *Curr. Opin. Struct. Biol.*, vol. 38, pp. 137–144, Jun. 2016.

[111] R. A. J. Darby, S. P. Cartwright, M. V. Dilworth, and R. M. Bill, “Which yeast species shall i choose? Saccharomyces cerevisiae versus Pichia pastoris (Review),” *Methods Mol. Biol.*, vol. 866, pp. 11–23, 2012.

[112] A. M. V. Gomes, T. S. Carmo, L. S. Carvalho, F. M. Bahia, and N. S. Parachin, “Comparison of Yeasts as Hosts for Recombinant Protein Production,” *Microorganisms*, vol. 6, no. 2, p. 38, Apr. 2018.

[113] A. Carlesso *et al.*, “Yeast as a tool for membrane protein production and structure determination,” *FEMS Yeast Res.*, vol. 22, no. 1, p. foac047, 2022.

[114] X. Li *et al.*, “Humanization of Yeasts for Glycan-Type End-Products,” *Front. Microbiol.*, vol. 13, p. 930658, Jul. 2022.

[115] E. J. Thak, S. J. Yoo, H. Y. Moon, and H. A. Kang, “Yeast synthetic biology for designed cell factories producing

secretory recombinant proteins," *FEMS Yeast Res.*, vol. 20, no. 2, Feb. 2020.

[116] F. Liu, X. Wu, L. Li, Z. Liu, and Z. Wang, "Use of baculovirus expression system for generation of virus-like particles: Successes and challenges," *Protein Expr. Purif.*, vol. 90, no. 2, p. 104, 2013.

[117] T. A. Kost, J. P. Condreay, and D. L. Jarvis, "Baculovirus as versatile vectors for protein expression in insect and mammalian cells," *Nat. Biotechnol.*, vol. 23, no. 5, p. 567, 2005.

[118] E. Ailor and M. J. Betenbaugh, "Modifying secretion and post-translational processing in insect cells," *Curr. Opin. Biotechnol.*, vol. 10, no. 2, pp. 142–145, Apr. 1999.

[119] A. L. Aloia, R. V. Glatz, E. J. McMurchie, and W. R. Leifert, "GPCR expression using baculovirus-infected Sf9 cells.," *Methods Mol. Biol.*, vol. 552, pp. 115–129, 2009.

[120] L. J. Olson and N. M. Dahms, "Cloning, Expression, and Purification of the Glycosylated Transmembrane Protein, Cation-Dependent Mannose 6-Phosphate Receptor, from Sf9 Cells Using the Baculovirus System," *Methods Mol. Biol.*, vol. 1722, p. 105, 2018.

[121] M. E. Linder, P. Middleton, J. R. Hepler, R. Taussig, A. G. Gilman, and S. M. Mumby, "Lipid modifications of G proteins: α subunits are palmitoylated," *Proc. Natl. Acad. Sci. U. S. A.*, vol. 90, no. 8, pp. 3675–3679, Apr. 1993.

[122] J. M. Kaipa, G. Krasnoselska, R. J. Owens, and J. van den Heuvel, "Screening of Membrane Protein Production by Comparison of Transient Expression in Insect and Mammalian Cells," *Biomolecules*, vol. 13, no. 5, p. 817, May 2023.

[123] N. Eifler *et al.*, "Functional expression of mammalian receptors and membrane channels in different cells," *J. Struct.*

Biol., vol. 159, no. 2, pp. 179–193, Aug. 2007.

[124] E. A. McKenzie and W. M. Abbott, “Expression of recombinant proteins in insect and mammalian cells,” *Methods*, vol. 147, pp. 40–49, Sep. 2018.

[125] S. Penuela, R. Bhalla, K. Nag, and D. W. Laird, “Glycosylation Regulates Pannexin Intermixing and Cellular Localization,” *Mol. Biol. Cell*, vol. 20, no. 20, p. 4313, Oct. 2009.

[126] B. Schneider *et al.*, “Membrane protein expression in cell-free systems.,” *Methods Mol. Biol.*, vol. 601, pp. 165–186, 2010.

[127] W. Gao, E. Cho, Y. Liu, and Y. Lu, “Advances and Challenges in Cell-Free Incorporation of Unnatural Amino Acids Into Proteins,” *Front. Pharmacol.*, vol. 10, no. MAY, p. 611, 2019.

[128] P. Wei *et al.*, “Cell-Free Expression of Unnatural Amino Acid Incorporated Aquaporin SS9 with Improved Separation Performance in Biomimetic Membranes,” *Biomed Res. Int.*, vol. 2018, no. 1, p. 3560894, Jan. 2018.

[129] Z. Köck *et al.*, “Cryo-EM structure of cell-free synthesized human histamine 2 receptor/Gs complex in nanodisc environment,” *Nat. Commun.*, vol. 15, no. 1, p. 1831, Dec. 2024.

[130] Z. Hajihassan, A. Ghaee, P. Bazargannia, and E. Salmani Shahrivar, “Affinity purification/immobilization of poly histidine-tagged proteins by nickel-functionalized porous chitosan membranes,” *J. Chromatogr. A*, vol. 1722, p. 464902, May 2024.

[131] N. Ayoub, P. Roth, Z. Ucurum, D. Fotiadis, and S. Hirschi, “Structural and biochemical insights into His-tag-induced higher-order oligomerization of membrane proteins by cryo-EM and size exclusion chromatography,” *J. Struct. Biol.*, vol.

215, no. 1, p. 107924, Mar. 2023.

[132] V. M. Bolanos-Garcia and O. R. Davies, "Structural analysis and classification of native proteins from E. coli commonly co-purified by immobilised metal affinity chromatography," *Biochim. Biophys. Acta - Gen. Subj.*, vol. 1760, no. 9, pp. 1304–1313, Sep. 2006.

[133] T. Kawate and E. Gouaux, "Fluorescence-Detection Size-Exclusion Chromatography for Precrystallization Screening of Integral Membrane Proteins," *Structure*, vol. 14, no. 4, pp. 673–681, 2006.

[134] S. Li, "Detergents and alternatives in cryo-EM studies of membrane proteins: Detergents and alternatives in cryo-EM studies of membrane proteins," *Acta Biochim. Biophys. Sin. (Shanghai).*, vol. 54, no. 8, p. 1049, 2022.

[135] J. W. GODING, "Analysis of Antigens Recognized by Monoclonal Antibodies," *Monoclon. Antibodies*, pp. 234–326, 1996.

[136] S. Hjertén, M. Sparrman, and J. li Liao, "Purification of membrane proteins in SDS and subsequent renaturation," *Biochim. Biophys. Acta - Biomembr.*, vol. 939, no. 3, pp. 476–484, Apr. 1988.

[137] P. J. Booth, S. L. Flitsch, L. J. Stern, D. A. Greenhalgh, P. S. Kim, and H. G. Khorana, "Intermediates in the folding of the membrane protein bacteriorhodopsin," *Nat. Struct. Biol.*, vol. 2, no. 2, pp. 139–143, 1995.

[138] B. C. Choy, R. J. Cater, F. Mancia, and E. E. Pryor, "A 10-year meta-analysis of membrane protein structural biology: Detergents, membrane mimetics, and structure determination techniques," *Biochim. Biophys. Acta - Biomembr.*, vol. 1863, no. 3, p. 183533, 2021.

[139] F. M. Menger, "The structure of micelles," *Acc. Chem. Res.*,

vol. 12, no. 4, pp. 111–117, 2002.

[140] F. Müh and A. Zouni, "Micelle formation in the presence of photosystem I," *Biochim. Biophys. Acta - Biomembr.*, vol. 1778, no. 10, pp. 2298–2307, Oct. 2008.

[141] B. T. Arachea, Z. Sun, N. Potente, R. Malik, D. Isailovic, and R. E. Viola, "Detergent selection for enhanced extraction of membrane proteins," *Protein Expr. Purif.*, vol. 86, no. 1, pp. 12–20, 2012.

[142] B. Chen *et al.*, "Coming Clean and Avoiding Bubble Trouble–Using Detergents Wisely in the Purification of Membrane Proteins for Cryo-EM Studies," *Biomolecules*, vol. 15, no. 9, p. 1315, Sep. 2025.

[143] V. Corradi *et al.*, "Emerging Diversity in Lipid–Protein Interactions," *Chem. Rev.*, vol. 119, no. 9, pp. 5775–5848, May 2019.

[144] Y. Gao, E. Cao, D. Julius, and Y. Cheng, "TRPV1 structures in nanodiscs reveal mechanisms of ligand and lipid action," *Nature*, vol. 534, no. 7607, pp. 347–351, May 2016.

[145] S. B. Long, X. Tao, E. B. Campbell, and R. MacKinnon, "Atomic structure of a voltage-dependent K+ channel in a lipid membrane-like environment," *Nature*, vol. 450, no. 7168, pp. 376–382, Nov. 2007.

[146] X. Chi, X. Li, Y. Chen, Y. Zhang, Q. Su, and Q. Zhou, "Cryo-EM structures of the full-length human KCC2 and KCC3 cation-chloride cotransporters," *Cell Res.*, vol. 31, no. 4, pp. 482–484, Apr. 2021.

[147] X. Yao, X. Fan, and N. Yan, "Cryo-EM analysis of a membrane protein embedded in the liposome," *Proc. Natl. Acad. Sci. U. S. A.*, vol. 117, no. 31, pp. 18497–18503, 2020.

[148] L. Wang and F. J. Sigworth, "Cryo-EM structure of the BK

potassium channel in a lipid membrane,” *Nature*, vol. 461, no. 7261, p. 292, Sep. 2009.

[149] L. Tonggu and L. Wang, “Broken symmetry in the human BK channel,” *bioRxiv*, p. 494385, Dec. 2018.

[150] H. H. Shen, T. Lithgow, and L. L. Martin, “Reconstitution of Membrane Proteins into Model Membranes: Seeking Better Ways to Retain Protein Activities,” *Int. J. Mol. Sci. 2013, Vol. 14, Pages 1589-1607*, vol. 14, no. 1, pp. 1589–1607, Jan. 2013.

[151] I. Siuda and D. P. Tieleman, “Molecular Models of Nanodiscs,” *J. Chem. Theory Comput.*, vol. 11, no. 10, pp. 4923–4932, 2015.

[152] I. G. Denisov and S. G. Sligar, “Nanodiscs in Membrane Biochemistry and Biophysics,” *Chem. Rev.*, vol. 117, no. 6, pp. 4669–4713, Mar. 2017.

[153] T. H. Bayburt and S. G. Sligar, “Membrane protein assembly into Nanodiscs,” *FEBS Lett.*, vol. 584, no. 9, pp. 1721–1727, May 2010.

[154] K. M. Strickland, K. Neselu, A. J. Grant, C. L. Espy, N. A. McCarty, and I. Schmidt-Krey, “Reconstitution of Detergent-Solubilized Membrane Proteins into Proteoliposomes and Nanodiscs for Functional and Structural Studies,” *Methods Mol. Biol.*, vol. 2302, pp. 21–35, 2021.

[155] T. K. Ritchie *et al.*, “Reconstitution of Membrane Proteins in Phospholipid Bilayer Nanodiscs,” *Methods Enzymol.*, vol. 464, no. C, pp. 211–231, Jan. 2009.

[156] M. A. Schuler, I. G. Denisov, and S. G. Sligar, “Nanodiscs as a new tool to examine lipid-protein interactions,” *Methods Mol. Biol.*, vol. 974, p. 415, 2013.

[157] M. Yokogawa, M. Fukuda, and M. Osawa, “Nanodiscs for

Structural Biology in a Membranous Environment," *Chem. Pharm. Bull. (Tokyo).*, vol. 67, no. 4, pp. 321–326, 2019.

[158] J. Frauenfeld *et al.*, "A saposin-lipoprotein nanoparticle system for membrane proteins," *Nat. Methods*, vol. 13, no. 4, pp. 345–351, 2016.

[159] A. Flayhan, H. D. T. Mertens, Y. Ural-Blimke, M. Martinez Molledo, D. I. Svergun, and C. Löw, "Saposin Lipid Nanoparticles: A Highly Versatile and Modular Tool for Membrane Protein Research," *Structure*, vol. 26, no. 2, pp. 345-355.e5, Feb. 2018.

[160] A. F. Craig *et al.*, "Tuning the size of styrene-maleic acid copolymer-lipid nanoparticles (SMALPs) using RAFT polymerization for biophysical studies," *Biochim. Biophys. Acta - Biomembr.*, vol. 1858, no. 11, pp. 2931–2939, Nov. 2016.

[161] T. J. Knowles, R. Finka, C. Smith, Y. P. Lin, T. Dafforn, and M. Overduin, "Membrane Proteins Solubilized Intact in Lipid Containing Nanoparticles Bounded by Styrene Maleic Acid Copolymer," *J. Am. Chem. Soc.*, vol. 131, no. 22, pp. 7484–7485, Jun. 2009.

[162] S. Vatsa, "In silico prediction of post-translational modifications in therapeutic antibodies," *MAbs*, vol. 14, no. 1, p. 2023938, 2022.

[163] S. Suraritdechachai, B. Lakkanasirorat, and C. Uttamapinant, "Molecular probes for cellular imaging of post-translational proteoforms," *RSC Chem. Biol.*, vol. 3, no. 2, p. 201, Feb. 2022.

[164] Z. Ruan, J. Du, and W. Lü, "Human Pannexin 1 Channel is NOT Phosphorylated by Src Tyrosine Kinase at Tyr199 and Tyr309," pp. 1–31, 2023.

[165] R. Aebersold and M. Mann, "Mass-spectrometric exploration

of proteome structure and function," *Nature*, vol. 537, no. 7620, pp. 347–355, Sep. 2016.

[166] J. V. Olsen and M. Mann, "Status of Large-scale Analysis of Post-translational Modifications by Mass Spectrometry," *Mol. Cell. Proteomics*, vol. 12, no. 12, p. 3444, Dec. 2013.

[167] Y. Jiang *et al.*, "Comprehensive Overview of Bottom-Up Proteomics Using Mass Spectrometry," *ACS Meas. Sci. Au*, vol. 4, no. 4, pp. 338–417, 2024.

[168] Y. Zhang, B. R. Fonslow, B. Shan, M. C. Baek, and J. R. Yates, "Protein Analysis by Shotgun/Bottom-up Proteomics," *Chem. Rev.*, vol. 113, no. 4, pp. 2343–2394, Apr. 2013.

[169] S. M. Chrysafides, S. J. Bordes, and S. Sharma, *Physiology, Resting Potential*. Treasure Island (FL): StatPearls Publishing, 2023.

[170] G. Dahl, "ATP release through pannexon channels," *Philos. Trans. R. Soc. B Biol. Sci.*, vol. 370, no. 1672, p. 20140191, Jul. 2015.

[171] I. C. Forster, K. Köhler, J. Biber, and H. Murer, "Forging the link between structure and function of electrogenic cotransporters: the renal type IIa Na+/Pi cotransporter as a case study," *Prog. Biophys. Mol. Biol.*, vol. 80, no. 3, pp. 69–108, Nov. 2002.

[172] S. Miyauchi *et al.*, "Sodium-coupled electrogenic transport of pyroglutamate (5-oxoproline) via SLC5A8, a monocarboxylate transporter," *Biochim. Biophys. Acta - Biomembr.*, vol. 1798, no. 6, pp. 1164–1171, 2010.

[173] A. Peres, S. Giovannardi, E. Bossi, and R. Fesce, "Electrophysiological Insights into the Mechanism of Ion-Coupled Cotransporters," *Physiology*, vol. 19, no. 2, pp. 80–84, Apr. 2004.

[174] M. Carter and J. C. Shieh, “Electrophysiology,” *Guid. to Res. Tech. Neurosci.*, pp. 91–118, 2010.

[175] N. Gamper, Ed., *Ion Channels*, Second., vol. 998. Totowa, NJ: Humana Press, 2013.

[176] R. Sherman-Gold, Ed., *The Axon Guide*, Third. 2012.

[177] G. Zhang and J. Cui, “Patch-Clamp and Perfusion Techniques to Study Ion Channels Expressed in Xenopus Oocytes,” *Cold Spring Harb. Protoc.*, vol. 2018, no. 4, pp. 258–267, Apr. 2018.

[178] W. Stühmer, “Electrophysiological recording from Xenopus oocytes,” *Methods Enzymol.*, vol. 207, no. C, pp. 319–339, Jan. 1992.

[179] L. Huang and C. Zhang, “Microscale Thermophoresis (MST) to Detect the Interaction Between Purified Protein and Small Molecule,” *Methods Mol. Biol.*, vol. 2213, pp. 187–193, 2021.

[180] D. Capelli, V. Scognamiglio, and R. Montanari, “Surface plasmon resonance technology: Recent advances, applications and experimental cases,” *TrAC Trends Anal. Chem.*, vol. 163, p. 117079, Jun. 2023.

[181] M. S. Smyth and J. H. J. Martin, “x Ray crystallography,” *J. Clin. Pathol. - Mol. Pathol.*, vol. 53, no. 1, pp. 8–14, 2000.

[182] J. M. Keith, Ed., *Bioinformatics*, vol. 452. Totowa, NJ: Humana Press, 2008.

[183] A. A. Kermani, “A guide to membrane protein X-ray crystallography,” *FEBS Journal*, vol. 288, no. 20. John Wiley and Sons Inc, pp. 5788–5804, 01-Oct-2021.

[184] M. Caffrey, “A comprehensive review of the lipid cubic phase or in meso method for crystallizing membrane and soluble proteins and complexes,” *Acta Crystallogr. Sect. F, Struct.*

Biol. Commun., vol. 71, no. Pt 1, p. 3, Jan. 2015.

[185] W. Gaisford, G. Schertler, and P. Edwards, “mosquito® LCP: Making membrane protein crystallization accessible to the research scientist,” *Nat. Methods 2011 86*, vol. 8, no. 6, pp. i–ii, May 2011.

[186] H. M. Berman *et al.*, “The Protein Data Bank,” *Nucleic Acids Res.*, vol. 28, no. 1, pp. 235–242, Jan. 2000.

[187] J. CAVANAGH, W. J. FAIRBROTHER, A. G. PALMER, M. RANCE, and N. J. SKELTON, “EXPERIMENTAL ASPECTS OF NMR SPECTROSCOPY,” *Protein NMR Spectrosc.*, pp. 114–270, 2007.

[188] D. Wishart, “NMR Spectroscopy and Protein Structure Determination: Applications to Drug Discovery and Development,” *Curr. Pharm. Biotechnol.*, vol. 6, no. 2, pp. 105–120, 2005.

[189] L. M. Epasto, K. Che, F. Kozak, A. Selimovic, P. Kaderavek, and D. Kurzbach, “Toward protein NMR at physiological concentrations by hyperpolarized water-Finding and mapping uncharted conformational spaces,” *Sci. Adv.*, vol. 8, no. 31, p. 5179, Aug. 2022.

[190] D. F. Gauto *et al.*, “Integrated NMR and cryo-EM atomic-resolution structure determination of a half-megadalton enzyme complex,” *Nat. Commun. 2019 101*, vol. 10, no. 1, pp. 1–12, Jun. 2019.

[191] S. Bibow and S. Hiller, “A guide to quantifying membrane protein dynamics in lipids and other native-like environments by solution-state NMR spectroscopy,” *FEBS Journal*, vol. 286, no. 9. Blackwell Publishing Ltd, pp. 1610–1623, 01-May-2019.

[192] E. Ruska, “The Development of the Electron Microscope and of Electron Microscopy (Nobel Lecture),” *Angew. Chemie Int.*

Ed. English, vol. 26, no. 7, pp. 595–605, 1987.

[193] D. B. Williams and C. B. Carter, *Transmission electron microscope*, 2nd ed. New York: Springer ScienceþBusiness Media, 2009.

[194] L. Metilli *et al.*, "Latest advances in imaging techniques for characterizing soft, multiphasic food materials," *Adv. Colloid Interface Sci.*, vol. 279, p. 102154, May 2020.

[195] N. Marturi, "Vision and visual servoing for nanomanipulation and nanocharacterization in scanning electron microscope," Université de FrancheComté, 2013.

[196] E. Y. D. Chua *et al.*, "Better, Faster, Cheaper: Recent Advances in Cryo–Electron Microscopy," *Annu. Rev. Biochem.*, vol. 91, p. 1, 2022.

[197] F. Houdellier, G. M. Caruso, S. Weber, M. Kociak, and A. Arbouet, "Development of a high brightness ultrafast Transmission Electron Microscope based on a laser-driven cold field emission source," *Ultramicroscopy*, vol. 186, pp. 128–138, Mar. 2018.

[198] G. McMullan, A. R. Faruqi, and R. Henderson, "Direct Electron Detectors," *Methods Enzymol.*, vol. 579, pp. 1–17, Jan. 2016.

[199] M. Ohi, Y. Li, Y. Cheng, and T. Walz, "Negative Staining and Image Classification – Powerful Tools in Modern Electron Microscopy," *Biol. Proced. Online*, vol. 6, no. 1, p. 23, Jan. 2004.

[200] P. L. Chiu, D. F. Kelly, and T. Walz, "The use of trehalose in the preparation of specimens for molecular electron microscopy," *Micron*, vol. 42, no. 8, p. 762, Dec. 2011.

[201] J. Dubochet and A. W. McDowall, "VITRIFICATION OF PURE WATER FOR ELECTRON MICROSCOPY," *J.*

Microsc., vol. 124, no. 3, pp. 3–4, Dec. 1981.

[202] P. Dubochet, J., Adrian, M., Chang, J., Homo, J., Lepault, J., McDowall, A., & Schultz, "Cryo-electron microscopy of vitrified specimens.," *Q. Rev. Biophys.*, vol. 21, no. 2, pp. 129–228, 1988.

[203] X. Mu, C. Gillman, C. Nguyen, and T. Gonen, "An Overview of Microcrystal Electron Diffraction (MicroED)," *Annual Review of Biochemistry*, vol. 90. pp. 431–450, 2021.

[204] A. Doerr, "Cryo-electron tomography," *Nature Methods*, vol. 14, no. 1. Nature Publishing Group, p. 34, 29-Dec-2016.

[205] Z. Wang and Q. Zhang, "Coming of Age : Cryo-Electron Tomography as a Versatile Tool to Generate High-Resolution Structures at Cellular / Biological Interfaces," 2021.

[206] R. N. Irobalieva, B. Martins, and O. Medalia, "Cellular structural biology as revealed by cryo-electron tomography," *J. Cell Sci.*, vol. 129, no. 3, pp. 469–476, 2016.

[207] M. Obr, W. J. H. Hagen, R. A. Dick, L. Yu, A. Kotecha, and F. K. M. Schur, "Exploring high-resolution cryo-ET and subtomogram averaging capabilities of contemporary DEDs," *J. Struct. Biol.*, vol. 214, no. 2, p. 107852, Jun. 2022.

[208] Y. Hong, Y. Song, Z. Zhang, and S. Li, "Cryo-Electron Tomography: The Resolution Revolution and a Surge of in Situ Virological Discoveries," *Annual Review of Biophysics*, vol. 52. pp. 339–360, 2023.

[209] T. Ni *et al.*, "High-resolution in situ structure determination by cryo-electron tomography and subtomogram averaging using emClarity," *Nature Protocols*, vol. 17, no. 2. Nature Publishing Group, pp. 421–444, 12-Jan-2022.

[210] R. I. Koning *et al.*, "Automated vitrification of cryo-EM samples with controllable sample thickness using suction and

real-time optical inspection,” *Nat. Commun. 2022 131*, vol. 13, no. 1, pp. 1–10, May 2022.

[211] J. Snijder *et al.*, “Vitrification after multiple rounds of sample application and blotting improves particle density on cryo-electron microscopy grids,” *J. Struct. Biol.*, vol. 198, no. 1, pp. 38–42, Apr. 2017.

[212] R. Kazan *et al.*, “Grid batch-dependent tuning of glow discharge parameters,” *Front. Mol. Biosci.*, vol. 9, p. 910218, Aug. 2022.

[213] I. Drulyte *et al.*, “Approaches to altering particle distributions in cryo-electron microscopy sample preparation,” *Acta Crystallogr. Sect. D, Struct. Biol.*, vol. 74, no. Pt 6, p. 560, Jun. 2018.

[214] T. S. Levitz *et al.*, “Approaches to Using the Chameleon: Robust, Automated, Fast-Plunge cryoEM Specimen Preparation,” *Front. Mol. Biosci.*, vol. 9, p. 903148, Jun. 2022.

[215] I. J. Hirst, W. J. R. Thomas, R. A. Davies, and S. P. Muench, “CryoEM grid preparation: a closer look at advancements and impact of preparation mode and new approaches,” *Biochem. Soc. Trans.*, vol. 52, no. 3, pp. 1529–1537, 2024.

[216] D. Ashtiani *et al.*, “Delivery of femtolitre droplets using surface acoustic wave based atomisation for cryo-EM grid preparation,” *J. Struct. Biol.*, vol. 203, no. 2, pp. 94–101, Aug. 2018.

[217] X. Feng *et al.*, “A Fast and Effective Microfluidic Spraying-plunging Method for High-Resolution Single-Particle Cryo-EM,” *Structure*, vol. 25, no. 4, p. 663, Apr. 2017.

[218] V. P. Dandey *et al.*, “Spotiton: New Features and Applications,” *J. Struct. Biol.*, vol. 202, no. 2, p. 161, May 2018.

[219] L. Rima *et al.*, "cryoWriter: a blotting free cryo-EM preparation system with a climate jet and cover-slip injector," *Faraday Discuss.*, vol. 240, no. 0, pp. 55–66, Nov. 2022.

[220] R. B. G. Ravelli *et al.*, "Cryo-EM structures from sub-nl volumes using pin-printing and jet vitrification," *Nat. Commun.*, vol. 11, no. 1, Dec. 2020.

[221] C. J. Russo and L. A. Passmore, "Ultrastable gold substrates: Properties of a support for high-resolution electron cryomicroscopy of biological specimens," *J. Struct. Biol.*, vol. 193, no. 1, pp. 33–44, Jan. 2016.

[222] R. S. Pantelic, J. C. Meyer, U. Kaiser, W. Baumeister, and J. M. Plitzko, "Graphene oxide: A substrate for optimizing preparations of frozen-hydrated samples," *J. Struct. Biol.*, vol. 170, no. 1, pp. 152–156, Apr. 2010.

[223] K. A. Taylor and R. M. Glaeser, "Retrospective on the early development of cryoelectron microscopy of macromolecules and a prospective on opportunities for the future," *J. Struct. Biol.*, vol. 163, no. 3, pp. 214–223, Sep. 2008.

[224] J. Chen, A. J. Noble, J. Y. Kang, and S. A. Darst, "Eliminating effects of particle adsorption to the air/water interface in single-particle cryo-electron microscopy: Bacterial RNA polymerase and CHAPSO," *J. Struct. Biol. X*, vol. 1, p. 100005, Jan. 2019.

[225] Y. Zi Tan *et al.*, "Addressing Preferred Specimen Orientation in Single-Particle Cryo-EM through Tilting," *Nat. Methods*, vol. 14, no. 8, p. 793, Jul. 2017.

[226] S. Rawson, M. G. Iadanza, N. A. Ranson, and S. P. Muench, "Methods to account for movement and flexibility in cryo-EM data processing," *Methods*, vol. 100, pp. 35–41, May 2016.

[227] A. Dhakal, R. Gyawali, L. Wang, and J. Cheng, "A large expert-curated cryo-EM image dataset for machine learning

protein particle picking," *Sci. Data*, vol. 10, no. 1, p. 392, Dec. 2023.

[228] A. F. Brilot *et al.*, "Beam-Induced Motion of Vitrified Specimen on Holey Carbon Film," *J. Struct. Biol.*, vol. 177, no. 3, p. 630, Mar. 2012.

[229] L. A. Baker and J. L. Rubinstein, "Radiation Damage in Electron Cryomicroscopy," *Methods Enzymol.*, vol. 481, no. C, pp. 371–388, Jan. 2010.

[230] Z. A. Ripstein and J. L. Rubinstein, "Processing of Cryo-EM Movie Data," *Methods Enzymol.*, vol. 579, pp. 103–124, Jan. 2016.

[231] L. A. Baker, E. A. Smith, S. A. Bueler, and J. L. Rubinstein, "The resolution dependence of optimal exposures in liquid nitrogen temperature electron cryomicroscopy of catalase crystals," *J. Struct. Biol.*, vol. 169, no. 3, pp. 431–437, Mar. 2010.

[232] S. Q. Zheng, E. Palovcak, J. P. Armache, K. A. Verba, Y. Cheng, and D. A. Agard, "MotionCor2: Anisotropic correction of beam-induced motion for improved cryo-electron microscopy," *Nat. Methods*, vol. 14, no. 4, pp. 331–332, Feb. 2017.

[233] J. Zivanov, T. Nakane, and S. H. W. Scheres, "A Bayesian approach to beam-induced motion correction in cryo-EM single-particle analysis," *urn:issn:2052-2525*, vol. 6, no. 1, pp. 5–17, Jan. 2019.

[234] S. H. Contreras Ortiz, T. Chiu, and M. D. Fox, "Ultrasound image enhancement: A review," *Biomed. Signal Process. Control*, vol. 7, no. 5, pp. 419–428, Sep. 2012.

[235] R. Bromberg, Y. Guo, D. Borek, and Z. Otwinowski, "CryoEM single particle reconstruction with a complex-valued particle stack," *J. Struct. Biol.*, vol. 215, no. 2, p. 107945, Jun.

2023.

[236] R. M. Tromp and S. M. Schramm, “Optimization and stability of the contrast transfer function in aberration-corrected electron microscopy,” *Ultramicroscopy*, vol. 125, pp. 72–80, Feb. 2013.

[237] E. D. Zhong, T. Bepler, B. Berger, and J. H. Davis, “CryoDRGN: reconstruction of heterogeneous cryo-EM structures using neural networks,” *Nat. Methods*, vol. 18, no. 2, pp. 176–185, 2021.

[238] G. Zanetti, J. D. Riches, S. D. Fuller, and J. A. G. Briggs, “Contrast transfer function correction applied to cryo-electron tomography and sub-tomogram averaging,” *J. Struct. Biol.*, vol. 168, no. 2–24, p. 305, Nov. 2009.

[239] T. Bendory, A. Bartesaghi, and A. Singer, “Single-Particle Cryo-Electron Microscopy,” 2017.

[240] Y. Cheng, “Single-particle cryo-EM at crystallographic resolution,” *Cell*, vol. 161, no. 3, p. 450, Apr. 2015.

[241] D. Tegunov and P. Cramer, “Real-time cryo-electron microscopy data preprocessing with Warp,” *Nat. Methods*, vol. 16, no. 11, pp. 1146–1152, 2019.

[242] A. Rohou and N. Grigorieff, “CTFFIND4: Fast and accurate defocus estimation from electron micrographs,” *J. Struct. Biol.*, vol. 192, no. 2, pp. 216–221, Nov. 2015.

[243] T. Bepler *et al.*, “Positive-unlabeled convolutional neural networks for particle picking in cryo-electron micrographs,” *Nat. Methods*, vol. 16, no. 11, pp. 1153–1160, Nov. 2019.

[244] T. Wagner *et al.*, “SPHIRE-crYOLO is a fast and accurate fully automated particle picker for cryo-EM,” *Commun. Biol.*, vol. 2, no. 1, pp. 1–13, Dec. 2019.

[245] N. P. Nguyen, I. Ersoy, J. Gotberg, F. Bunyak, and T. A. White, “DRPnet: automated particle picking in cryo-electron micrographs using deep regression,” *BMC Bioinformatics*, vol. 22, no. 1, pp. 1–28, Dec. 2021.

[246] A. Heimowitz, J. Andén, and A. Singer, “APPLE picker: Automatic particle picking, a low-effort cryo-EM framework,” *J. Struct. Biol.*, vol. 204, no. 2, p. 215, Nov. 2018.

[247] D. Tegunov, L. Xue, C. Dienemann, P. Cramer, and J. Mahamid, “Multi-particle cryo-EM refinement with M visualizes ribosome-antibiotic complex at 3.5 Å in cells,” *Nat. Methods*, vol. 18, no. 2, pp. 186–193, Feb. 2021.

[248] T. Moriya *et al.*, “Size matters: optimal mask diameter and box size for single-particle cryogenic electron microscopy,” *bioRxiv*, p. 2020.08.23.263707, 2020.

[249] J. Frank, *Three-Dimensional Electron Microscopy of Macromolecular Assemblies*. Oxford University Press, 2006.

[250] S. H. W. Scheres *et al.*, “Disentangling conformational states of macromolecules in 3D-EM through likelihood optimization,” *Nat. Methods*, vol. 4, no. 1, pp. 27–29, 2007.

[251] F. J. Sigworth, “A Maximum-Likelihood Approach to Single-Particle Image Refinement,” *J. Struct. Biol.*, vol. 122, no. 3, pp. 328–339, Jan. 1998.

[252] S. H. W. Scheres, “Processing of Structurally Heterogeneous Cryo-EM Data in RELION,” *Methods Enzymol.*, vol. 579, pp. 125–157, Jan. 2016.

[253] S. H. W. Scheres *et al.*, “Maximum-likelihood Multi-reference Refinement for Electron Microscopy Images,” *J. Mol. Biol.*, vol. 348, no. 1, pp. 139–149, Apr. 2005.

[254] A. Punjani, J. L. Rubinstein, D. J. Fleet, and M. A. Brubaker, “CryoSPARC: Algorithms for rapid unsupervised cryo-EM

structure determination," *Nat. Methods*, vol. 14, no. 3, pp. 290–296, Feb. 2017.

[255] S.-C. Chung, H.-H. Lin, K.-P. Wu, T.-L. Chen, W.-H. Chang, and I.-P. Tu, "RE2DC: a robust and efficient 2D classifier with visualization for processing massive and heterogeneous cryo-EM data," *bioRxiv*, p. 2022.11.21.517443, Nov. 2022.

[256] D. A. Semchonok, F. L. Kyrilis, F. Hamdi, and P. L. Kastritis, "Cryo-EM of a heterogeneous biochemical fraction elucidates multiple protein complexes from a multicellular thermophilic eukaryote," *J. Struct. Biol. X*, vol. 8, p. 100094, Dec. 2023.

[257] P. A. Penczek, "Fundamentals of three-dimensional reconstruction from projections," *Methods Enzymol.*, vol. 482, no. C, p. 1, 2010.

[258] E. Levin, T. Bendory, N. Boumal, J. Kileel, and A. Singer, "3D ab initio modeling in cryo-EM by autocorrelation analysis," *Proc. - Int. Symp. Biomed. Imaging*, vol. 2018-April, pp. 1569–1573, May 2018.

[259] J. Zivanov *et al.*, "New tools for automated high-resolution cryo-EM structure determination in RELION-3," *Elife*, vol. 7, Nov. 2018.

[260] A. Punjani, H. Zhang, and D. J. Fleet, "Non-uniform refinement: adaptive regularization improves single-particle cryo-EM reconstruction," *Nat. Methods 2020 1712*, vol. 17, no. 12, pp. 1214–1221, Nov. 2020.

[261] S. H. W. Scheres, "A Bayesian View on Cryo-EM Structure Determination," *J. Mol. Biol.*, vol. 415, no. 2, pp. 406–418, Jan. 2012.

[262] S. H. W. Scheres and S. Chen, "Prevention of overfitting in cryo-EM structure determination," *Nat. Methods*, vol. 9, no. 9, pp. 853–854, Sep. 2012.

[263] P. B. Rosenthal and R. Henderson, "Optimal Determination of Particle Orientation, Absolute Hand, and Contrast Loss in Single-particle Electron Cryomicroscopy," *J. Mol. Biol.*, vol. 333, no. 4, pp. 721–745, Oct. 2003.

[264] M. Van Heel and M. Schatz, "Fourier shell correlation threshold criteria," *J. Struct. Biol.*, vol. 151, no. 3, pp. 250–262, Sep. 2005.

[265] P. K. Singh and T. M. Iverson, "Improving CryoEM maps of symmetry-mismatched macromolecular assemblies: A case study on the flagellar motor," *J. Struct. Biol.*, vol. 217, no. 2, p. 108184, Jun. 2025.

[266] A. Punjani and D. J. Fleet, "3D variability analysis: Resolving continuous flexibility and discrete heterogeneity from single particle cryo-EM," *J. Struct. Biol.*, vol. 213, no. 2, p. 107702, Jun. 2021.

[267] J. He, T. Li, and S. Y. Huang, "Improvement of cryo-EM maps by simultaneous local and non-local deep learning," *Nat. Commun.*, vol. 14, no. 1, pp. 1–16, Dec. 2023.

[268] S. Kaur *et al.*, "Local computational methods to improve the interpretability and analysis of cryo-EM maps," *Nat. Commun. 2021 121*, vol. 12, no. 1, pp. 1–12, Feb. 2021.

[269] E. Ramírez-Aportela *et al.*, "Automatic local resolution-based sharpening of cryo-EM maps," *Bioinformatics*, vol. 36, no. 3, pp. 765–772, Feb. 2020.

[270] A. Bharadwaj, R. de Bruin, and A. J. Jakobi, "Confidence-guided cryo-EM map optimisation with LocScale-2.0," *bioRxiv*, p. 2025.09.11.674726, Sep. 2025.

[271] R. Sanchez-Garcia, J. Gomez-Blanco, A. Cuervo, J. M. Carazo, C. O. S. Sorzano, and J. Vargas, "DeepEMhancer: a deep learning solution for cryo-EM volume post-processing," *Commun. Biol.*, vol. 4, no. 1, pp. 1–8, Dec. 2021.